

**SUSTAINABLE TREATMENT OF PERCHLORATE
CONTAMINATED WATER**

by

Johanna Faccini

A THESIS SUBMITTED IN PARTIAL FULFILLMENT OF

THE REQUIREMENTS FOR THE DEGREE OF

MASTER OF APPLIED SCIENCE

in

The College of Graduate Studies

(Civil Engineering)

THE UNIVERSITY OF BRITISH COLUMBIA

(Okanagan)

July 2011

© Johanna Faccini, 2011

ABSTRACT

Perchlorate is a stable and soluble substance that can last for decades in the environment. Studies have shown that it can reduce iodine uptake into the thyroid gland which is of concern for people with decreased iodine intake, pregnant women and small children. Perchlorate is removed from drinking water using highly selective ion exchange (IX) resins that are replaced after exhaustion and incinerated or disposed in a landfill since there are no viable methods for regenerating them. One of the major limitations in regeneration of these single use resins is achieving complete desorption of perchlorate.

The sustainability of treatment processes for perchlorate contaminated water can be achieved by regenerating the exhausted resin. A study on the adsorption and desorption equilibrium, kinetics and biological regeneration of perchlorate from a trybutylamine strong base anion (SBA) exchange resin was conducted. Adsorption and desorption equilibrium could be described using the Freundlich model with estimated parameters $K_F = 50 \text{ (mg/g)(L/mg)}^{1/n}$ and $n = 2.36$. The calculated average perchlorate-chloride separation factor was 4700 ± 1700 and the resin capacity was 1.4 meq/mg. The kinetics of adsorption and desorption of perchlorate from the resin were found to be controlled by chemisorption since a pseudo-second order rate model fit the data the best.

The results from the physical/chemical studies were then applied to model the biological regeneration of the resin using the culture NP30. Experiments conducted with the exhausted resin inside a membrane to avoid direct contact with the culture, demonstrated the biological regeneration of the resin by degradation of the desorbed

perchlorate. The model was able to describe the desorption and biodegradation of perchlorate from the exhausted resin and the results were comparable to the experimental data. The model was found to be sensitive to the Freundlich adsorption intensity parameter n .

TABLE OF CONTENTS

ABSTRACT	ii
TABLE OF CONTENTS	iv
LIST OF TABLES	vii
LIST OF FIGURES	viii
LIST OF ACRONYMS, SYMBOLS AND ABBREVIATIONS	xi
ACKNOWLEDGMENTS	xiv
CHAPTER 1 INTRODUCTION	1
CHAPTER 2 LITERATURE REVIEW	3
2.1 Background	3
2.1.1 Perchlorate Occurrence	3
2.1.2 Physicochemical Properties of Perchlorate	4
2.1.3 Perchlorate Toxicity and Regulations	5
2.1.4 Remediation Technologies	6
2.2 Ion Exchange for Perchlorate Remediation	7
2.2.1 Principles	7
2.2.2 Ion Exchange Systems for Perchlorate Removal	11
2.2.3 Equilibrium and Separation Factors	13
2.3 Biological Perchlorate Treatment	16
2.3.1 Perchlorate Biodegradation from High Salt Solutions.	16
2.3.2 Salt-Tolerant Perchlorate Reducing Cultures	17
2.3.3 Direct Biodegradation of Perchlorate on Resins	19
2.4 Principles of Mass Transport on Porous Solids	20

2.4.1 Diffusion.....	22
2.4.2 Adsorption Kinetic Models.....	24
2.4.2.1 Adsorption Reaction Models.....	25
2.4.2.2 Adsorption Diffusion Models.....	28
2.5 Operating Diagrams.....	32
CHAPTER 3 MATERIALS AND METHODS.....	35
3.1 Resin Conditioning.....	35
3.2 Column Resin Exhaustion.....	36
3.3 Sorption Isotherms.....	38
3.4 Separation Factor.....	39
3.5 Sorption Kinetics.....	40
3.6 Biological Regeneration of Exhausted Resin.....	42
3.6.1 Resin Exhaustion.....	42
3.6.2 Media Preparation.....	42
3.6.3 Inoculum Source.....	43
3.6.4 Biological Regeneration of Exhausted Resin.....	44
3.7 Analytical Methods.....	45
3.7.1 Ion Chromatography.....	45
3.7.2 Perchlorate Probe.....	45
CHAPTER 4 RESULTS.....	47
4.1 Resin Capacity.....	47
4.2 Equilibrium Studies.....	50
4.2.1 Separation Factor.....	56
4.3 Kinetic Studies.....	57

4.3.1 Adsorption Studies.....	58
4.3.2 Desorption Studies.....	61
4.4 Mass Transport and Diffusion.....	65
4.4.1 Diffusion Controlled Sorption Studies	65
4.4.2 Adsorption Kinetic Models.....	69
4.4.2.1 Pseudo-First Order Kinetic Model.....	69
4.4.2.2 Pseudo-Second Order Kinetic Model	70
4.4.2.3 Elovich’s Equation.....	72
4.4.2.4 Second-Order Rate Equation	73
4.4.2.5 Film Diffusion Mass Transfer Rate	75
4.4.2.6 Weber-Morris Model	76
4.4.2.7 Dumwald-Wagner Model	77
4.4.2.8 Boyd Kinetic Model	78
4.4.3 Desorption Kinetic Models.....	81
4.5 Biological Regeneration of Exhausted Resin.....	86
CHAPTER 5 CONCLUSIONS AND FUTURE STUDY	96
5.1 Future Studies	98
REFERENCES	99
APPENDIX A	107
APPENDIX B.....	108

LIST OF TABLES

Table 2-1	Physical and chemical properties of perchlorate salts ^a	5
Table 3-1	La Puente concentration of ions.....	37
Table 3-2	Input data for EMCT simulation.....	38
Table 3-3	Composition of 6% synthetic medium prepared for culture NP30.....	43
Table 4-1	Capacities of commercial perchlorate selective IX resins.....	49
Table 4-2	EMCT predicted results.....	50
Table 4-3	Freundlich model parameters of SBA resins.....	56
Table 4-4	Parameters of adsorption reaction kinetic models applied to the adsorption of perchlorate onto loose resin experiments.....	75
Table 4-5	Parameters of adsorption diffusion models applied to the adsorption of perchlorate onto loose resin experiments.....	80
Table 4-6	Parameters of kinetic models applied to the desorption of perchlorate from the resin inside the membrane.....	86

LIST OF FIGURES

Figure 2-1	Perchlorate ion structure and dimensions.....	4
Figure 2-2	a) Styrene (STY) and b) divinylbenzene (DVB) structures.	8
Figure 2-3	Cross-linked polystyrene.....	8
Figure 2-4	Gel and microporous structures of ion exchange resins.....	9
Figure 2-5	Types of SBA resins a) Type I and b) Type II.....	10
Figure 2-6	Ion exchange systems used for perchlorate removal from drinking water.....	12
Figure 2-7	Four stages of adsorption into a porous solid.....	21
Figure 2-8	Operating diagram of a desorption process from a resin with an initial concentration q_0	33
Figure 3-1	N-butyl amine functional group of the studied resin.....	35
Figure 3-2	Serum bottles with resin in 100 mL solution for sorption isotherm test.	39
Figure 3-3	Set up for kinetics adsorption experiments of resin inside the membrane...41	
Figure 4-1	Column exhaustion breakthrough of ClO_4^- for La Puente water composition, 2 mL/min flow rate and 20°C.....	48
Figure 4-2	Freundlich isotherms for samples equilibrated during 1 day and 1 week at 20°C.....	51
Figure 4-3	Langmuir isotherms for samples equilibrated during 1 day and 1 week at 20°C.....	52
Figure 4-4	Comparison of 24 hours and one week equilibrium sorption isotherms. Samples taken at 20°C.....	53
Figure 4-5	Adsorption and desorption isotherm for samples taken at 20°C after 24 hours of equilibration. Desorption on 6% NaCl.....	54
Figure 4-6	Freundlich equilibrium sorption isotherms at 20°C. Data averaged for 24 hours and 1 week, adsorption and desorption for each mass of resin tested.....	55

Figure 4-7	Comparison of sorption kinetics resin loose and inside membrane data presented for 60 minutes at 20°C.	59
Figure 4-8	Comparison adsorption kinetics loose resin and in membrane data presented for 72 hours at 20°C.	60
Figure 4-9	Comparison of adsorption and desorption of perchlorate on 2.00 and 3.00 g of loose resin at 20°C. C_0 is initial perchlorate concentration of adsorption experiment.	62
Figure 4-10	Comparison of adsorption and desorption of perchlorate on 2.00 and 3.00 g of resin inside the membrane at 20°C. C_0 is the initial perchlorate concentration of the adsorption experiments.	63
Figure 4-11	Comparison of adsorption and desorption of perchlorate on 2.00 and 3.00 g of resin loose and inside the membrane at 20°C.	64
Figure 4-12	Experimental and fitted results of perchlorate adsorption on loose resin during the first 60 minutes. The fitted lines plot the analytical solutions obtained by trial and error of the diffusion coefficient.	66
Figure 4-13	Experimental and fitted results of perchlorate adsorption on loose resin during the first 1440 minutes (24hr). The fitted lines plot the analytical solutions obtained by trial and error of the diffusion coefficient.	67
Figure 4-14	Experimental and fitted results of perchlorate desorption on loose resin during the first 60 minutes. The fitted lines plot the analytical solutions obtained by trial and error of the diffusion coefficient.	68
Figure 4-15	Pseudo-first order kinetics of perchlorate adsorption onto loose resin.	70
Figure 4-16	Pseudo-second order kinetics of adsorption of perchlorate onto loose resin.	72
Figure 4-17	Elovich's model of adsorption of perchlorate onto loose resin.	73
Figure 4-18	Second order kinetics of adsorption of perchlorate onto loose resin.	74
Figure 4-19	Film diffusion mass transfer rate model of adsorption of perchlorate onto loose resin.	76
Figure 4-20	Weber-Morris model of adsorption of perchlorate onto loose resin.	77
Figure 4-21	Dumwald-Wagner model of adsorption of perchlorate onto loose resin.	78
Figure 4-22	Boyd kinetic model of adsorption of perchlorate onto loose resin.	79

Figure 4-23	Pseudo-second order rate model of desorption of perchlorate from resin inside the membrane and 6% NaCl solution.	83
Figure 4-24	Boyd kinetic model of perchlorate desorption from resin inside the membrane and 6% NaCl solution.....	85
Figure 4-25	Biological degradation experimental set up.	87
Figure 4-26	Biological regeneration of exhausted SBA resin using NP30 culture at 20°C. One replicate was killed after sampling. Initially seven replicates....	88
Figure 4-27	Operating diagram of the biological degradation process of perchlorate desorbed from the resin.	90
Figure 4-28	Model and experimental results for the desorption and biological regeneration of perchlorate exhausted resin contained inside a membrane.	92
Figure 4-29	Operating diagram of the modeled biological regeneration of perchlorate desorbed from the resin.	93
Figure 4-30	Reactor design for the biological regeneration of perchlorate exhausted resin.	95

LIST OF ACRONYMS, SYMBOLS AND ABBREVIATIONS

DVB	Divinylbenzene
FBR	Fluidized bed reactor
IX	Ion exchange
PRB	Perchlorate-reducing bacteria
SBA	Strong base anionic
SBR	Sequencing batch reactor
STY	Styrene
WBA	Weak base anionic
a	Elovich's equation desorption constant (mg/g/min),
Bi	Biot number,
B	Boyd kinetic model parameter ($B=\pi^2D_i/r^2$) (1/min),
C	adsorbate concentration in the solution or in the pores of the resin at time t (mg/L), (mg/L),
C_{Cl^-}	chloride equilibrium concentration in the solution (meq/L),
$C_{ClO_4^-}$	perchlorate equilibrium concentration in the solution (meq/L),
C_T	total solution concentration (meq/L),
Ce	adsorbate or perchlorate equilibrium concentration in the solution (mg/L),
C_i	initial concentration of adsorbate or perchlorate (meq/L),
C_t	adsorbate concentration in the solution at time t (mg/L),
D	adsorbate diffusion coefficient within the porous media (cm^2/min),
D_e^1	effective liquid film diffusion coefficient (cm^2/min),

D_i	effective diffusion coefficient (cm^2/min),
F	fraction of adsorbate in the resin at time t (unitless),
Fo	Fourier number ($Fo = D \cdot t/r^2$) (unitless),
g	mass of dry resin (g),
k	film diffusion mass transfer rate equation equilibrium constant (min^{-1}),
K	intraparticle diffusion rate equation constant of adsorption (min^{-1}),
k_{d2}	pseudo-second order rate constant for the desorption kinetic model (g/mg/min),
K_F	Freundlich adsorption capacity parameter ($\text{mg/g})(\text{L/mg})^{1/n}$,
k_f	mass transfer coefficient (cm/min),
K_L	equilibrium constants of Langmuir equation,
k_{p1}	pseudo-first order rate constant for the kinetic model (min^{-1}),
k_{p2}	pseudo-second order rate constant for the kinetic model (g/mg/min),
K_s	half saturation constant ($\text{mg ClO}_4^-/\text{L}$),
M	mass of resin (g),
n	Freundlich adsorption intensity parameter (unitless),
q	adsorbate concentration in the resin (mg/g),
q_{Cl^-}	chloride equilibrium concentration in the resin (meq/g resin),
$q_{ClO_4^-}$	perchlorate equilibrium concentration in the resin (meq/g resin),
q_e	adsorbate concentrations in the resin at equilibrium (mg/g),
q_{ecal}	kinetic model parameter (mg/g),
Q_e	perchlorate equilibrium concentration in the resin (mg/g),
q_0	initial concentration of adsorbate in the resin (mg/g),
q_t	adsorbate concentrations in the resin at time t (mg/g),

Q_T	total equilibrium concentration in the resin or resin capacity (meq/g resin),
r	distance from the center of the particle (cm),
R^l	liquid film diffusion constant (min^{-1}),
r_o	particle radius (cm),
S	substrate concentration (mg/L),
t	time (min),
V	volume of solution in the reactor (L),
X	biomass concentration (mg VSS/L),
X_{Cl^-}	fraction of chloride in the solution phase,
$X_{ClO_4^-}$	fraction of perchlorate in the solution phase,
Y	biomass yield (mg VSS/ mg ClO_4^-),
Y_{Cl^-}	fraction of chloride in the resin phase.
$Y_{ClO_4^-}$	fraction of perchlorate in the resin phase,
α	Elovich's equation initial adsorption rate (mg/q/min),
α_L	equilibrium constants of Langmuir equation,
Δr_o	thickness of the liquid film (cm),
λ	roots of Biot equation,
v	specific perchlorate reduction rate ($ClO_4^-/\text{mg VSS}\cdot\text{h}$),
v_m	maximum specific perchlorate reduction rate (mg $ClO_4^-/\text{mg VSS}\cdot\text{h}$),

ACKNOWLEDGMENTS

I would like to thank Dr. Deborah Roberts, for her support, guidance and patience. I truly appreciate her understanding at the time when my circumstances slowed the progress of this work. Without her advice this work would have not been culminated successfully.

I am also grateful to Dr. C. Eskicioglu, Dr. V. Prodanovic and Dr. J. Curtis for taking time out their busy schedules to review this work and serve on my committee.

I am truly thankful to Yeyuan (Roger) Xiao for his directions with the use of the Ion Chromatograph and help manipulating the culture and sampling. I wish you success in all your future endeavors.

To my parents Emilio and Concha and my parents in law Antonio and Alma all my admiration and love, I could not have taken this journey without you coming this far to assist us with our daily routines so I could have the time to complete this project.

Finally to my husband Antonio my most profound appreciation, there are no words to express my love for you. Your strength and loving care keeps me going, thanks for being always there for me. My children Sofia and Tomás so cheerful and alive, I adore you both, thanks for being such inspiration. Now we can play more “pet shops” and “pirates and mermaids”.

CHAPTER 1 INTRODUCTION

Perchlorate (ClO_4^-) is a very stable and soluble substance that can last for many decades in surface and ground water (Wang et al., 2008; Yoon et al., 2008; Motzer, 2001). Studies have shown that it can reduce iodine uptake into the thyroid gland which is of concern for people with decreased iodine intake, pregnant women and small children (Urbansky, 1998; US EPA, 2005a).

Highly selective ion exchange (IX) resins are currently used for removing perchlorate from contaminated drinking water. Single use IX resins are replaced after exhaustion and exhausted resins are disposed of by incineration or landfill disposal since there are no viable methods for regenerating the resin. Although the run times of these resins are in the order of tens of thousands of bed volumes (Aldridge et al., 2004), the new resins cost up to \$1500/cubic foot. Highly concentrated NaCl solutions (6-12 %) can be used to desorb perchlorate from the exhausted IX resins (Sutton, 2006; Lehman et al., 2008; Van Ginkel et al., 2008; Tripp, 2001, ATSDR, 2008). Research has shown that a University of British Columbia Okanagan salt-tolerant perchlorate-reducing culture in direct contact with the resin is capable of degrading perchlorate to chloride and oxygen (Xiao et al., 2009).

The purpose of this project was to study the behavior of adsorption and desorption of perchlorate onto a strong base anion (SBA) exchange resin. Gaining knowledge of the equilibrium, sorption kinetics and biological degradation was important to develop a

model to describe the combined process of desorption and biological regeneration of the resin.

The research goal was attained through studies organized as follows:

- Determination of resin capacity using a breakthrough curve.
- Determination of resin equilibrium model and parameters.
- Study of perchlorate adsorption and desorption using the SBA resin.
- Determination of kinetic models and parameters.
- Study of biological regeneration of perchlorate desorbed from the exhausted resin.

The ability to model the process would allow for designing a system to regenerate the exhausted resin reducing the costs associated with the new resin and its disposal; which in turn, would ultimately constitute a significant development to convert the treatment of perchlorate contaminated water into a more sustainable operation.

CHAPTER 2 LITERATURE REVIEW

2.1 Background

2.1.1 Perchlorate Occurrence

Manmade perchlorate is manufactured to be used mainly in defense and aerospace sectors as an oxidizing agent for solid propellant rockets, missiles and munitions (Motzer, 2001; Urbansky, 2002). Manmade perchlorate salts can also be found in several applications such as highway safety flares, fireworks, pyrotechnics, explosives, common batteries, and automobile restrain systems (DTSC, 2007). About 90% of manmade perchlorate is in the form of ammonium perchlorate, other manufactured salts include sodium and potassium perchlorate.

Perchlorate (ClO_4^-) occurs naturally in Chilean caliche ore deposits which are mined and processed to produce a fertilizer rich in sodium nitrate (NaNO_3). The fertilizer was sold in the USA for the tobacco, cotton, citrus fruits and vegetable crops (Urbansky et al. 2001). An interesting fact about perchlorate occurrence is that its presence is not only limited to Earth, it also occurs on Mars. Perchlorate salts (sodium and magnesium) have been detected in considerable amounts (~1 wt %) in Mars' arctic (Zorzano et al., 2009; NASA, 2008).

Since the spring of 1997, perchlorate has been recurrently found in soil, surface and ground water in 49 states of the United States, the District of Columbia and Puerto Rico (US, EPA, 2010). This increased detection is due to advances in analytical techniques

capable of detecting low perchlorate contamination levels (< 50 ppb) in 1997 (Urbansky, 2000). The areas of the United States with the highest number of contaminated sites are Massachusetts, southern California, west central Texas, New Jersey, and the Long Island coast (ITRC, 2008). As for Canada, a preliminary ground and surface water analysis performed by Health Canada showed that perchlorate levels in the country are extremely low or non-existent (Health Canada, 2008).

2.1.2 Physicochemical Properties of Perchlorate

The perchlorate anion is made up of one chlorine atom surrounded by four oxygen atoms in a tetrahedral array as shown in Figure 2-1. The ion has a low charge density and is kinetically inert to reduction resulting in a non-complexing anion that poorly adsorbs to mineral or organic surfaces (Brown et al., 2006; Urbansky, 2002).

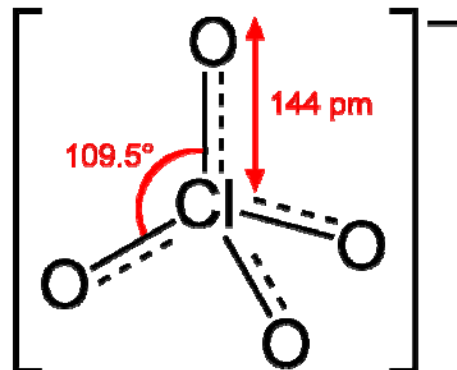


Figure 2-1 Perchlorate ion structure and dimensions.

Perchlorate forms odorless, colorless and highly soluble salts, with ammonium, magnesium, potassium, sodium and lithium being the most common. Table 2-1 summarizes the physicochemical properties of the salts.

Table 2-1 Physical and chemical properties of perchlorate salts^a.

Property	Magnesium perchlorate	Potassium perchlorate	Ammonium perchlorate	Sodium perchlorate	Lithium perchlorate
Chemical formula	Mg(ClO ₄) ₂	KClO ₄	NH ₄ ClO ₄	NaClO ₄	LiClO ₄
Molar mass (g/mol)	223.21	138.55	117.49	122.44	106.39
Colour	White	Colourless or white	White crystals	White	Colourless crystals
Physical state	Solid granular flaky powder	Solid crystals	Solid crystals	Solid deliquesce crystals	Solid crystals
Melting point (°C)	-250	400	130	471	236
Solubility (mg/L)	9.96x10 ⁵	2.06x10 ⁴	2.49x10 ⁵	2.10x10 ⁶	5.97x10 ⁵

^a Adapted from ATSDR, 2008.

Due to its high solubility in water and kinetic stability, perchlorate is very difficult to remove from water effectively. Once it is introduced into the environment, perchlorate is expected to be very recalcitrant and mobile in surface and groundwater and it may exist in the environment for many decades (Wang et al., 2008; Yoon et al., 2008; Motzer, 2001)

2.1.3 Perchlorate Toxicity and Regulations

One study (Urbansky, 1998) has shown that perchlorate affects thyroid hormone function by reducing iodine uptake into the thyroid gland. Concern remains regarding the long term effects of low thyroid hormones on individuals with decreased iodine intake especially pregnant women and children (US EPA, 2005a). On January 2009, the USEPA

issued an interim drinking water health advisory level of 15 µg/L (USEPA, 2009), the Office of Environmental Health Hazard Assessment in California set a Public Health Goal (PHG) of perchlorate in drinking water of 6 µg/L (OEHA, 2009), and Massachusetts has set a goal of 2 µg/L. Health Canada (2008), has recommended a drinking water guidance of 6 µg/L based on other agencies health risk assessments.

2.1.4 Remediation Technologies

There are several technologies that can remove perchlorate contamination from drinking water including biological reduction, reverse osmosis, electrodialysis, nanofiltration, biological treatments and IX treatments (Bowman 2004; Matos et al., 2006; Lehman, 2008). Currently ion exchange is the most prevalent technology in use, due to its high removal efficiency, its simplicity and capability at relatively high flow rates with a small footprint (Van Ginkel et al., 2008; Yoon et al., 2008).

Reverse osmosis, electrodialysis and nanofiltration are effective at removing perchlorate but are expensive and generate perchlorate concentrated brine solutions that require treatment before disposal (Matos et al., 2006; Chung et al., 2007). Currently biological treatment and ion exchange are the only technologies with commercial scale applications. Perchlorate removal by IX has been favoured over other technologies because the exhausted resin can be regenerated and reused and it also removes other contaminant ions such nitrate and sulfate (Sutton, 2006; Lehman et al., 2008).

Biological treatment uses perchlorate-reducing bacteria capable of degrading perchlorate to the chloride ion (Cl^-) and oxygen at low cost, but application of biological systems to drinking water treatment is restricted due to concerns about the health effects of bacteria and their by-products (Lehman et al., 2008, Matos et al., 2006). Therefore, biological treatment has been applied indirectly to treat spent brines produced from other treatments, rather than directly to drinking water.

2.2 Ion Exchange for Perchlorate Remediation

2.2.1 Principles

Ion exchange (IX) is a process that involves the replacement of ions from a fluid (usually an aqueous solution) with dissimilar ions of similar charge using a solid matrix with the opposite charge. The solid is usually a porous polymer that contains permanently bound functional groups (Perry and Green., 1999). Most IX resins are made of cross-linked styrene (STY) and divinylbenzene (DVB), shown in Figure 2-2; which imparts insolubility and toughness to the resin (Wachinski et al., 1997), the higher the DVB amount the higher the toughness, which is defined as the ability of the material to withstand a load before fracturing.



Figure 2-2 a) Styrene (STY) and b) divinylbenzene (DVB) structures.

Figure 2-3 presents a scheme of polystyrene cross-linking, the link is made by introducing DVB into the structure. As the amount of DVB increases, the size of the pores within the resin decreases which can negatively affect how large ions enter the resin and thus their removal, as in a gel type ion exchange resin. Macroporous resins overcome this issue by having artificial porosity in the tri-dimensional matrix that is created during the polymerization process.

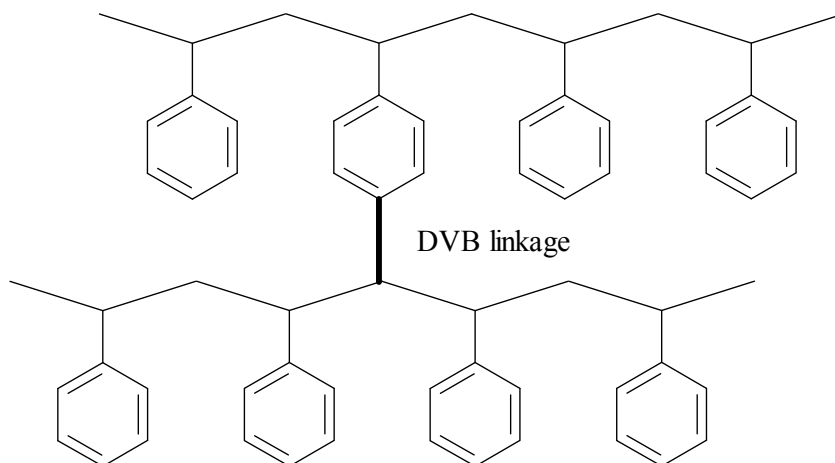


Figure 2-3 Cross-linked polystyrene.

Figure 2-4 represents the two types of structures: gel and macroporous. Gel type resins have 4% to 10% cross-linking and macroporous have 20% to 25%. As a result, macroporous resins possess large surface areas (7 to 600 m²/g) and porosities of 20% to 60% (MWH, 2005). Ion exchange selectivity is also a function of the resin porosity. In general terms the higher the ion valence, the higher the removal by a resin. However, the degree of cross-linking changes the relative affinity of the resin for certain ions relative to the chloride anion, and as a function of the functional groups attached to the resin matrix.

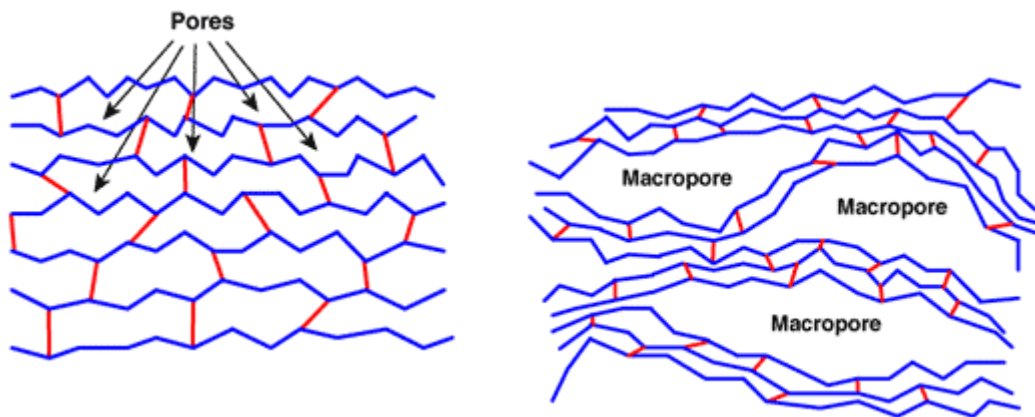


Figure 2-4 Gel and microporous structures of ion exchange resins.

(Source: http://dardel.info/IX/resin_structure.html)

IX resins used for perchlorate removal are divided in two categories depending on the functional group attached to the resin matrix: strong base anionic resins (SBA) with quaternary ammonium functional groups and weak base anionic resins (WBA) with secondary or tertiary amines as functional groups (Xiong et al., 2007; Wachinski et al., 1997).

SBA resins are further divided in two types based on the functional group. In type I three alkyl (methyl, ethyl, propyl, butyl) groups are bonded to the quaternary amine. In type II an ethanol group replaces one of the alkyl groups as shown in Figure 2-5.

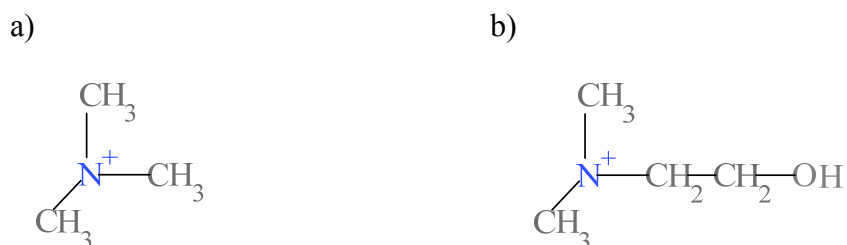


Figure 2-5 Types of SBA resins a) Type I and b) Type II.

Type I resins have greater chemical stability and Type II have slightly greater regeneration efficiency and capacity (Wachinski et al., 1997; MWH, 2005). SBA resins are usually operated in the chloride form and regenerated with NaCl.

According to work by Tripp and Clifford (2006), perchlorate selectivity is significantly controlled by the type of resin matrix and the type of functional group attached to it. They showed that polystyrenic (more hydrophobic) resins present higher affinities for perchlorate than polyacrylic type resins. Perchlorate displays higher affinity for IX resins with macroporous hydrophobic matrices since it is a large ion (58.8 cm³/g-mole) classified as poorly hydrated (Batista et al., 2002).

Another important characteristic of IX resins is the particle size. In commercially available resins the particle diameter ranges from 0.04 to 1.0 mm. This is relevant because IX kinetics are proportional to the inverse of the square of the particle diameter

and also because smaller particles increase pressure drops across an IX column which affects the column hydraulics and design.

2.2.2 Ion Exchange Systems for Perchlorate Removal

Currently there are two types of IX systems available for removing perchlorate from drinking water, regenerable and single use. Figure 2-6 presents a flow chart that depicts the regenerable and single use type of systems. The regenerable system uses perchlorate selective WBA or non selective SBA resins. The advantages of this system are the capability of reusing the resin and the requirement for small regenerant volumes (< 0.02% of treated water) due to the fact that WBA are pH dependant. At low pH they are protonated and can exchange ions but at higher pH the resin becomes uncharged and can be regenerated. SBA can be regenerated with high concentrations of NaCl.

The disadvantages of this system are the use of sodium chloride brine of concentration ranging from 6% to saturation or the need to adjust the pH of the treated water before and after IX by the addition of chemicals. Additionally the disposal of spent regenerant solution becomes a challenge because of the high sodium chloride concentration and the presence of perchlorate, nitrate, sulfate and even arsenic anions (Van Ginkel et al., 2008; Tripp, 2001, ATSDR, 2008).

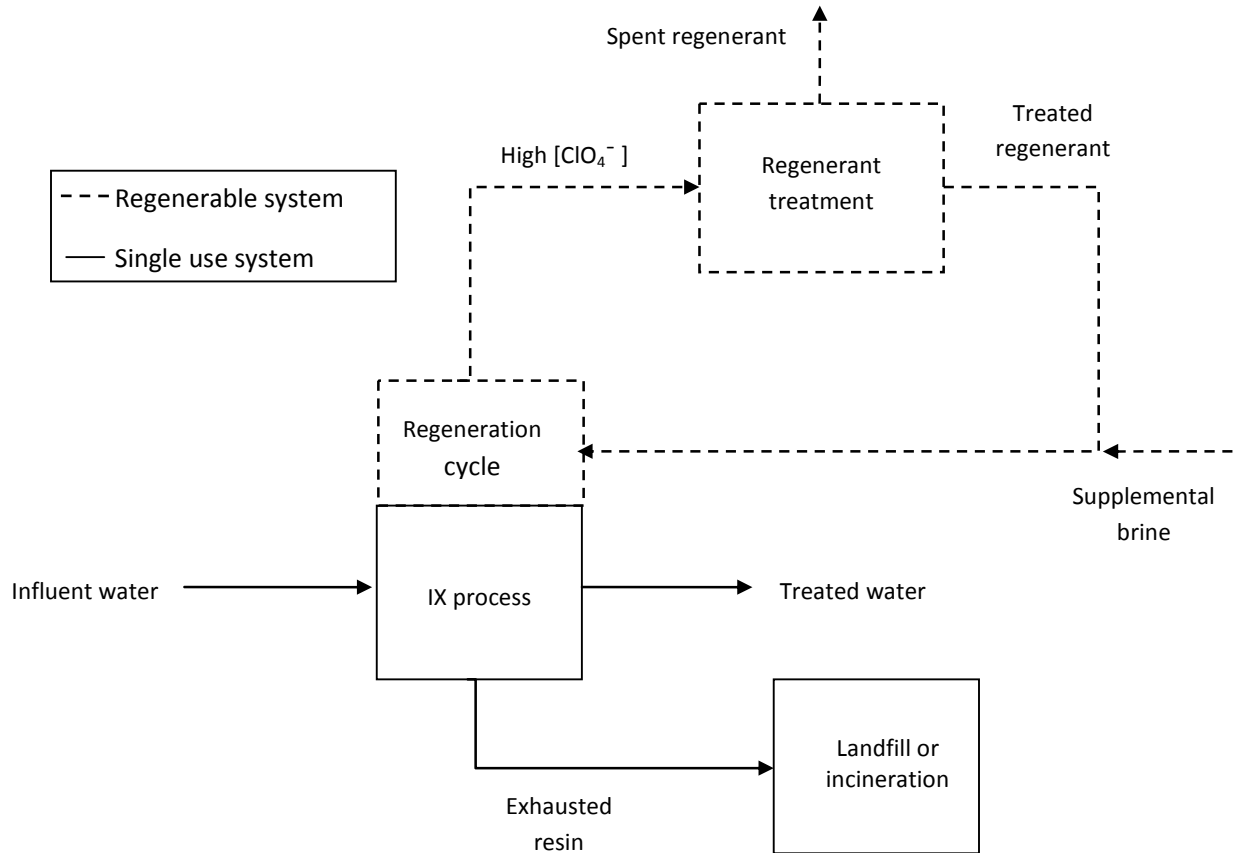


Figure 2-6 Ion exchange systems used for perchlorate removal from drinking water.

Single use IX systems use highly selective SBA resins that bind perchlorate so tightly that is not feasible to regenerate them. However the large number of bed volumes of water treated at very low perchlorate concentrations before breakthrough makes them an attractive choice (Venkatesan et al., 2010; ATSDR, 2008). The disadvantage of the single use IX resins relies in the management of spent resins which includes landfill and incineration. Landfill disposal is not widely used since it requires analysis for waste classification and perchlorate is not destroyed. Incineration by thermal destruction

eliminates perchlorate but also the costly IX resin after a single use which makes the process unsustainable (ATSDR, 2008).

2.2.3 Equilibrium and Separation Factors

Models used to describe the proportioning of ions between the aqueous and resin phases in IX include Langmuir, Freundlich and multi-ion chromatography. Equilibrium isotherms describe the distribution of perchlorate between the liquid and solid phases at constant temperature when there is no net transfer of perchlorate between the phases. Isotherms also provide a way of evaluating the transport mechanisms and parameters involved in the IX process. The abundance and accessibility of adsorption sites that affect isotherm results are dependent on pore size distribution, tortuosity and functional group.

Isotherm models attained from analysis of experimental equilibrium data provide valuable information for process design (Abdullah et al., 2009). Langmuir and Freundlich isotherm models shown in equations 2-1 and 2-2 respectively are the most commonly used in the literature.

$$q_e = \frac{K_L C_e}{1 + \alpha_L C_e}, \quad 2-1$$

where:

C_e is the perchlorate equilibrium concentration in the solution (mg/L),

q_e is the perchlorate equilibrium concentration in the resin (mg/g),

K_L and α_L are the equilibrium constants of Langmuir equation (unitless),

$$q_e = K_F C_e^{1/n}, \quad 2-2$$

where:

K_F is the Freundlich adsorption capacity parameter $(\text{mg/g})(\text{L/mg})^{1/n}$,

$1/n$ is the Freundlich adsorption intensity parameter, unitless.

The Freundlich adsorption isotherm model has been found to better represent the experimental data in several studies of perchlorate adsorption onto activated carbon and perchlorate selective IX resins such SR-7, CalRes 2103, A-530E, IRA-900, SRI-110 (Yoon, et al., 2008; Xiong et al., 2007; Hristovski et al., 2008).

The expression below presents the exchange of perchlorate on SBA Type I tributylamine resin (the one used in this project) with chloride:



The separation factor defines the preference for the perchlorate ion over the chloride ion during IX process and can be expressed as:

$$\alpha_{Cl^-}^{ClO_4^-} = \frac{Y_{ClO_4^-} X_{Cl^-}}{Y_{Cl^-} X_{ClO_4^-}}, \quad 2-4$$

where the unitless parameters are:

$X_{ClO_4^-}$ is the fraction of perchlorate in the solution phase,

X_{Cl^-} is the fraction of chloride in the solution phase,

$Y_{ClO_4^-}$ is the fraction of perchlorate in the resin phase,

Y_{Cl^-} is the fraction of chloride in the resin phase.

The fractions on each phase are calculated as:

$$X_{ClO_4^-} = \frac{C_{ClO_4^-}}{C_T}, \quad 2-5$$

$$X_{Cl^-} = \frac{C_{Cl^-}}{C_T}, \quad 2-6$$

$$Y_{ClO_4^-} = \frac{q_{ClO_4^-}}{Q_T}, \quad 2-7$$

$$Y_{Cl^-} = \frac{q_{Cl^-}}{Q_T}, \quad 2-8$$

where:

$C_{ClO_4^-}$ is the perchlorate equilibrium concentration in the solution (meq/L),

C_{Cl^-} is the chloride equilibrium concentration in the solution (meq/L),

C_T is the total solution concentration (meq/L),

$q_{ClO_4^-}$ is the perchlorate equilibrium concentration in the resin (meq/g resin),

q_{Cl^-} is the chloride equilibrium concentration in the resin (meq/g resin),

Q_T is the total equilibrium concentration in the resin or resin capacity (meq/g resin).

The separation factor would be greater than unity if the resin shows more affinity for perchlorate than for chloride. For process design, the separation factor is determined experimentally (Tripp, 2001; MWH, 2005) and it would not necessarily be a constant. Factors that could affect the separation factor include the size and charge of the ions, resin particle size, degree of cross-linking, capacity, type of functional group, as well as the total concentration of the solution and temperature. Tripp (2001) studied the influence of temperature for a number of resins concluding that an increase in temperature decreased the resins preference for perchlorate over chloride and that the effect of chloride concentration in the solution had no significant effect on the IX process. Separation factors are usually derived from experimental data of binary ion exchange isotherms.

2.3 Biological Perchlorate Treatment

2.3.1 Perchlorate Biodegradation from High Salt Solutions.

Several studies have shown the feasibility of using perchlorate-reducing bacteria for the biological regeneration of perchlorate after ion exchange treatment. The majority of studies focus on treating the regenerant brine and only a few studies deal with the direct

biological regeneration of the exhausted resin (Xiao et al., 2010; Vankatesan et al., 2010) but there is growing interest in this option.

The process involves employing salt-tolerant perchlorate-reducing bacteria (PRB) capable of decomposing perchlorate loaded into the resin. Sequencing batch reactors (SBR) and fluidized bed reactors (FBR) are the two types of processes that have been tested. Salt-tolerant PRB has been tested for treating highly concentrated regenerant brines. Hiremath et al. (2006) demonstrated that PRB could degrade 4.3 mg/L of perchlorate within 24 hours in brine with 5.3 – 10% NaCl. The salt-tolerant culture was also tested by Kashyap (2006) to regenerate perchlorate loaded resins Amberlite IRA-996 and Ionac SR-7 by direct contact in an SBR. The author showed that bacteria were capable of reducing the available perchlorate in solution in 2 hours. The desorption of perchlorate from the resin was shown to be the rate limiting step, taking up to 40 hours for a complete desorption in 6% NaCl medium. As a drawback, the author noted that separation of resin and biomass once the regeneration was completed was a tedious task.

2.3.2 Salt-Tolerant Perchlorate Reducing Cultures

Perchlorate reducing bacteria (PRB) have been found in diverse environments (soil, water, marine water/sediment, and groundwater) but very few are salt-tolerant (Coates et al., 1999). Chung et al. (2009) reported results of a perchlorate and nitrate reducing bacteria identified as *Clostridium sp.* and *Rhodocyclaceae* species as the dominant clones that might be tolerant to high salinity. Cang et al. (2004) developed a salt-tolerant PRB from marine sediment inoculated in March 2000 in a 3% NaCl medium and fed acetate as

electron donor and perchlorate as electron acceptor. This culture, named FP30, was capable of reducing nitrate and perchlorate in solutions of 3 to 6% NaCl. By 2003 a new culture NP30 was started from FP30 in 3% NaCl media. A study showed that NP30 is capable of reducing 4.3 mg/L of perchlorate in brine below detection limits within 24 hours from samples collected at La Puente County Water District's IX process (Hiremath et al., 2006). In research by Lehman et al. (2008), the culture NP30 was used in a SBR to treat spent brine from a pilot IX system. The authors showed that NP30 was capable of reducing perchlorate below the treatment goal of 500 µg/L in 6% NaCl. A study using a FBR to treat synthetic brine (6% NaCl) in a column inoculated with NP30 over granulated activated carbon (GAC) as support medium concluded that perchlorate reduction from 300 mg/L to 2 mg/L was achieved. A different study in a pilot scale FBR using NP30 identified the perchlorate reducing bacteria in NP30 culture as *Azoarcus* and *Denitromonas* by denaturing gradient gel electrophoresis (DGGE) and fluorescent in situ hybridization (FISH) tests (Xiao et al., 2010).

Zuo, (2008) studied culture NP30 and found that the degradation rate can be described by saturation type substrate utilization model:

$$v = \frac{v_m S}{K_s + S}, \quad 2-9$$

where:

v is the specific perchlorate reduction rate (mg ClO₄⁻/mg VSS·h),

v_m is the maximum specific perchlorate reduction rate ($\text{mg ClO}_4^-/\text{mg VSS}\cdot\text{h}$),

K_s is the half saturation constant ($\text{mg ClO}_4^-/\text{L}$),

S is the substrate concentration (mg/L).

With a half saturation coefficient of $26 \pm 2 \text{ mg/L}$ and maximum reduction rate $(4.3 \pm 0.41) \times 10^{-3} \text{ mg ClO}_4^-/\text{mg VSS}\cdot\text{h}$.

2.3.3 Direct Biodegradation of Perchlorate on Resins

Research on biodegradation of IX resins in direct contact with the PRB cultures have been published by Xiao et al. (2010); Venkatesan et al. (2010), and Wang et al. (2008). These authors agree that biological regeneration of perchlorate laden IX resins is essential for an economical and sustainable treatment of perchlorate contaminated water with highly selective resins.

Xiao et al. (2010) developed a numerical analysis of direct biological regeneration in batch reactors using an inoculum from NP30 in 6% NaCl to treat resins IRA-996 and Ionac SR-7. The data collected allowed the authors to develop a model based on desorption kinetics, the degradation of perchlorate and the bacterial growth. The study concluded that the separation factor has a significant effect on the time to complete regeneration, the higher the separation factor, the shorter the time. The author also analyzed the biodegradation and desorption process concluding that degradation took

place in the concentrated liquid film around the resin and in the bulk aqueous phase (Xiao et al., 2010).

2.4 Principles of Mass Transport on Porous Solids

Mass transport of material across a solid-liquid interface can be described in terms of the resistance to mass transfer from each of the phases. Therefore it is important to understand the nature and magnitude of these resistances (Perry and Green, 1999). Resistance to mass transport from each one of the phases creates a concentration gradient that constitutes the driving force. The mass transfer rate can be expressed as proportional to the difference in the bulk concentration and the concentration at the interface which are assumed to be in equilibrium.

Adsorption from the bulk of the solution onto a porous solid can be described as four consecutive stages as represented in Figure 2-7 (Plazinski and Rudzinski, 2010; Baup et al., 2000, Koopal et al., 2001; MWH, 2005).

The adsorbate is first transported from the bulk of the liquid solution by means of convection towards the liquid film encircling the porous particle. The concentration of adsorbate in the liquid bulk is a function of the overall mass balance and hydraulics of the reactor and appears to be a fast convective process compared to the mass transfer that takes place in the liquid film (Baup et al., 2000). Transport in the liquid film is characterized by the mass transfer coefficient k_f that depends on the type of flow

surrounding the particle, some physical properties of the solvent such polarity, viscosity and density and the molecular diffusion of the adsorbate.

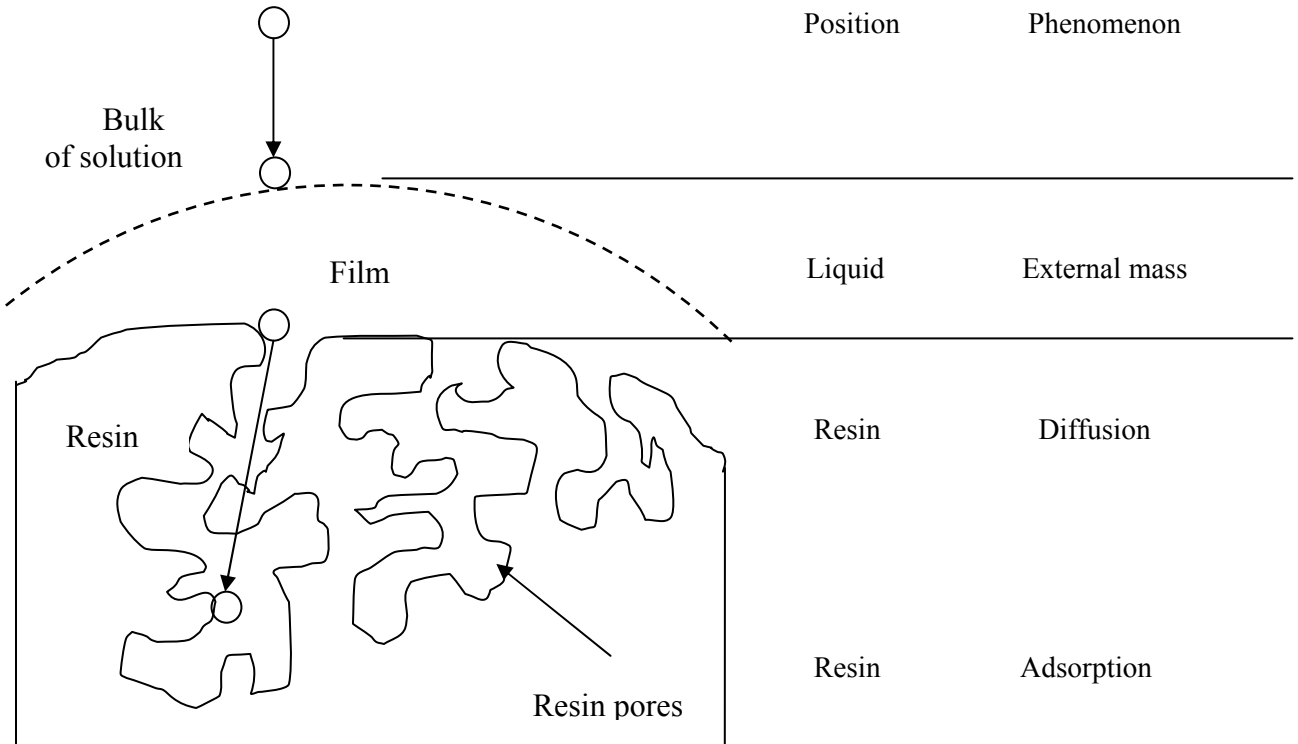


Figure 2-7 Four stages of adsorption into a porous solid.

The mass transfer coefficient k_f is related to the liquid film thickness and varies with fluid mixing. In the case of complete mixing the mass transfer resistance in the liquid film is minimized and the third stage, intraparticle diffusion becomes the main resistance to transport (Gomes, et al., 2001; MWH, 2005). The last stage is adsorption onto the resin surface and it can be considered a type of chemical reaction due to electrostatic attraction between the surface and adsorbate ions (Koopal et al., 2001; Plazinski and Rudzinski,

2009; Chiarle et al., 2000, Xie et al., 2009). Depending on which stage proceeds at a much slower rate than the other, the process can be either controlled by the transport or by the chemical reaction. If both rates are similar then both mechanisms control the adsorption process (Koopal et al., 2001).

2.4.1 Diffusion

In many cases adsorption is controlled by intraparticle diffusion rates. Several studies on a number of IX resins and GAC have shown that diffusion in the resin pores is usually the most important factor controlling mass transport (Baup et al., 2000; Gomes et al., 2001; Perry and Green, 1999; Plazinski and Rudzinski, 2009; Sonetaka et al., 2009; Xiong et al., 2007). The description of intraparticle diffusion is based on Fick's laws of diffusion that for the particular case of unsteady state in spherical particles is defined by equation 2-10,

$$\frac{\partial C}{\partial t} = D \left[\frac{1}{r^2} \frac{\partial}{\partial r} \left(r^2 \frac{\partial C}{\partial r} \right) \right], \quad \text{2-10}$$

where:

C is the adsorbate concentration in the pores of the resin at time t (mg/L),

t is time (min),

D is the adsorbate diffusion coefficient within the porous media (cm²/min),

r is the distance from the center of the particle (cm).

For initial conditions of uniform mass distribution and boundary conditions of central symmetry and convective boundary at the surface, the analytical solution to equation 2-10 is:

$$\frac{C - C_e}{C_i - C_e} = \sum_{n=1}^{\infty} \left[\frac{6}{\lambda_n^3} \frac{(\sin \lambda_n - \lambda_n \cos \lambda_n)^2}{\lambda_n - \sin \lambda_n \cos \lambda_n} e^{(-\lambda_n^2 Fo)} \right], \quad \mathbf{2-11}$$

where:

C_e is the equilibrium concentration of adsorbate (mg/L),

C_i is the initial concentration of adsorbate (mg/L),

Fo is Fourier number ($Fo = D \cdot t / r^2$) dimensionless.

λ are the roots of equation 2-11 that depends on the geometry and for the case of a sphere is:

$$Bi = \frac{1 - \lambda}{\tan \lambda} = \frac{k_f \times r}{D}, \quad \mathbf{2-12}$$

where:

Bi is the Biot number,

k_f is the mass transfer coefficient (cm/min).

As seen in equation 2-12, the Biot number provides a relationship between the intraparticle diffusion resistance and external resistance to mass transfer. The hydraulics of the process can be controlled so the resistance of the liquid film to mass transfer is reduced by agitation. Researchers have obtained results from batch experiments comparable to analytical solutions where the diffusion is the dominant resistance (Sonetaka, 2009). In the case of $Fo > 0.2$ the use of the first term of equation 2-11 provides acceptable solutions (Yovanovich, 2010; Erdoğan, 2005) and can be rewritten in the form of equation 2-13

$$\frac{C - C_e}{C_i - C_e} = \frac{6}{\pi^2} e^{(-\pi^2 Fo)} \quad \mathbf{2-13}$$

2.4.2 Adsorption Kinetic Models

The ion exchange process is carried out in a closed vessel by contacting the IX resin with the solution to be treated. Batch adsorption experiments carried out in this fashion are the most common method for studying adsorption equilibrium and kinetics. Data collected from the experiments can be modeled to determine the factors controlling the adsorption rate and common isotherm models (Langmuir and Freundlich) can be used to evaluate equilibrium as well.

The prediction of kinetics is important for the prediction of adsorption rates and provides information for designing and modeling (Guo et al., 2009). Models applied to describe the kinetic process of adsorption can be classified as adsorption reaction models (based on the chemical reaction) and adsorption diffusion models (based on the mass transfer) (Qiu et al. 2009; Ho, 2006). Adsorption diffusion models are defined based on the four stages presented in the previous section (convection, external mass transfer, diffusion and adsorption onto the surface). On the other hand, adsorption reaction models originate from chemical reaction kinetics and have also been widely used to describe experimental adsorption data (Ho, 2006; Qiu et al., 2009; Guo, 2009).

2.4.2.1 Adsorption Reaction Models

Pseudo-first order rate equation: Proposed by Lagergren (1898), this model describes liquid-solid adsorption kinetics. To distinguish kinetic equations based on adsorption capacity from solution concentration, Lagergren's equation has been called pseudo-first order (Ho, 2006). It has been widely used for describing the adsorption of pollutants from aqueous solutions (Ho, 2006).

$$\frac{dq_t}{dt} = k_{p1}(q_e - q_t), \quad \mathbf{2-14}$$

Integrated with boundary conditions of $t=0$ to $t=t$ and $q=0$ to $q=q_t$ yields:

$$\log(q_e - q_t) = \log q_e - \frac{k_{p1}}{2.303} t, \quad \mathbf{2-15}$$

where:

q_t is the adsorbate concentrations in the resin at time t (mg/g),

q_e is the adsorbate concentrations in the resin at equilibrium (mg/g),

k_{p1} is the pseudo-first order rate constant for the kinetic model (min^{-1}).

Pseudo-second order rate equation: This model was proposed by Ho in 1995 to describe the adsorption of divalent metal ions onto peat. The assumptions were that adsorption could be described by a second order equation and that chemical adsorption was the rate limiting step due to the exchange of electrons between the peat and divalent metal ions (Qiu et al., 2009). The equation describing the adsorption rate is given as:

$$\frac{dq_t}{dt} = k_{p2}(q_e - q_t)^2. \quad \mathbf{2-16}$$

According to Ho (2006), the driving force ($q_e - q_t$) is proportional to the available fraction of active sites. Rearranging and integrating equation 2-16 with boundary conditions $q_t=0$ at $t=0$ and $q_t=q_t$ at $t=t$ yields:

$$\frac{t}{q_t} = \frac{1}{q_e} t + \frac{1}{k_{p2}q_e^2}, \quad \mathbf{2-17}$$

where:

k_{p2} is the pseudo-second order rate constant for the kinetic model (g/mg/min).

A plot of t/q_t against time can be used to determine the initial adsorption rate $h=k_p2q_e^2$ (mg/g/min). According to Ho (2006), the pseudo-second order equation is used to describe chemisorption as sharing or exchange of electrons between the adsorbent and adsorbate as covalent forces and ion exchange.

Elovich's equation: Established by Zeldowitsch in 1934, this model describes the kinetic law of chemisorption from studies of the rate of adsorption of carbon monoxide on manganese dioxide. It has been applied to describe the kinetics of adsorption of gases onto heterogeneous solids and lately the adsorption of pollutants from aqueous solutions on highly heterogeneous adsorbents (Ho, 2006; Kumar et al., 2011). The Elovich equation is presented as:

$$\frac{dq_t}{dt} = ae^{-\alpha q}, \quad \text{2-18}$$

where:

a is the desorption constant (unitless),

α is the initial adsorption rate (unitless).

Once rearranged to a linear form and for the case of $\alpha at \gg 1$, the integrated equation yields:

$$q_t = \alpha \ln(a \alpha) + \alpha \ln(t), \quad \text{2-19}$$

Second-order rate equation: Blanchard in 1984 conducted studies on the adsorption of NH_4^+ ions fixed into zeolite by divalent metallic ions in solution and presented a second-order rate equation assuming that the metallic concentration changes slightly during the first hours. This equation has been used to describe the exchange process of copper, cadmium and nickel from solutions with sodium ions from zeolite (Ho, 2006). The typical second-order rate equation is:

$$\frac{dC_t}{dt} = -k_2(C_t)^2, \quad \text{2-20}$$

Integration of 2-20 with the boundary conditions of $C_t=0$ at $t=0$ and $C_t=C_t$ at $t=t$ results in:

$$\frac{1}{C_t} = k_2 t + \frac{1}{C_e}, \quad \text{2-21}$$

where:

C_t is the adsorbate concentration in the solution at time t (mg/L),

C_e is the adsorbate concentration in the solution at equilibrium (mg/L).

2.4.2.2 Adsorption Diffusion Models

These models deal with the four stages of adsorption: transport in the bulk of the solution, diffusion across the liquid film, particle diffusion in the resin pores and sorption within the particle surface. The controlling mechanism could be any of these stages or a combination of steps. Evidence that chemisorption kinetics could be the controlling

mechanism is provided by modeling the experimental data with the pseudo-second order rate equation (Ho et al., 2010; Qui et al., 2009; Ho, 2006) that was described in the previous section, film diffusion and particle diffusion models are presented below.

Film diffusion mass transfer rate equation: presented by Boyd et al., in 1947 this model was successfully applied to the adsorption of phenol by a polymeric adsorbent NDA-100 and nickel(II) onto cashew nut shell (Qiu et al., 2009; Kumar et al., 2011) and expressed as:

$$\ln \left[1 - \frac{q_t}{q_e} \right] = -R^l t, \quad \text{2-22}$$

$$R^l = \frac{3D_e^l}{r_o \Delta r_o k}, \quad \text{2-23}$$

where:

R^l is the liquid film diffusion constant (min^{-1}),

D_e^l is the effective liquid film diffusion coefficient (cm^2/min),

r_o is the particle radius (cm),

Δr_o is the thickness of the liquid film (cm),

k is the equilibrium constant of adsorption (min^{-1}).

Equation 2-22 would be in the same form of the pseudo-first order equation 2-15 if the logarithm was used instead of the natural logarithm. This indicates that differentiating between film diffusion and pseudo-first order reaction is rather difficult (Ho et al., 2010).

Intraparticle diffusion models: The model equations for describing the adsorption as controlled by the diffusion of adsorbate into the adsorbent pores are: Weber-Morris model, Dumwald-Wagner model, and Boyd kinetic model.

The intraparticle diffusion model called Weber-Morris describes adsorption rates for which the solute uptake varies proportionally with $t^{1/2}$ as presented in equation 2-24. In this model it is essential that the plot of q versus $t^{1/2}$ goes through the origin if intraparticle diffusion is the sole mechanism controlling the adsorption rate.

$$q_t = k_{int}t^{1/2} + C. \quad \text{2-24}$$

Another intraparticle diffusion model is called the Dumwald-Wagner and was proposed as:

$$F = \frac{q_t}{q_e} = 1 - \frac{6}{\pi^2} \sum_{n=1}^{\infty} \frac{1}{n^2} e^{(-n^2 Kt)}, \quad \text{2-25}$$

where:

K is the rate constant of adsorption (min^{-1}),

F is the fraction of adsorbate in the resin at time t (unitless).

Equation 2-25 can be simplified to:

$$\log(1 - F^2) = -\frac{K}{2.303} t. \quad \mathbf{2-26}$$

This has been proven for the adsorption of *p*-toluidine onto a hypercrosslinked polymeric adsorbent. A plot of $\log(1 - F^2)$ vs t should be linear with slope K .

The Boyd kinetic model allows the distinction between film diffusion and particle diffusion and was presented by Boyd et al., in 1947 as:

$$F = \frac{q_t}{q_e} = 1 - \frac{6}{\pi^2} e^{(-Bt)}, \quad \mathbf{2-27}$$

where:

Bt is a mathematical function of F .

Arranging equation 2-27 and taking the natural logarithm to obtain equation 2-28:

$$Bt = -0.4977 - \ln(1 - F). \quad \mathbf{2-28}$$

A linear plot of the experimental data of Bt versus t that also passes through the origin is an indication that intraparticle diffusion is the controlling mechanism of adsorption. The effective diffusion coefficient D_i (cm^2/min) can then be estimated from the following equation:

$$B = \frac{\pi^2 D_i}{r^2},$$

2.5 Operating Diagrams

Operating diagrams are plots of the adsorbate concentration in the liquid phase as a function of the adsorbate concentration in the resin phase and consist of two lines: an equilibrium line and an operating line (MWH, 2005). The diagrams can be used to determine the minimum amount of resin required for a treatment and the size of the reactor. The operating line is derived from the mass balance in the batch reactor. For the case of desorption of an adsorbate from an exhausted resin in solution:

$$C = \frac{M}{V}(q_o - q), \quad \text{2-30}$$

where:

C is the adsorbate concentration in the solution (mg/L),

M is the mass of resin (g),

V is the volume of solution in the reactor (L),

q_o is the initial concentration of adsorbate in the resin (mg/g),

q is the adsorbate concentration in the resin (mg/g).

The operating diagram is a representation of equation 2-30 and is shown in Figure 2-8. In the diagram the slope of the operation line is $-M/V$ and the driving force is $(q_o -$

q_e). At a time t , the concentration of adsorbate in the solid and liquid phase is represented by q_t and C_t .

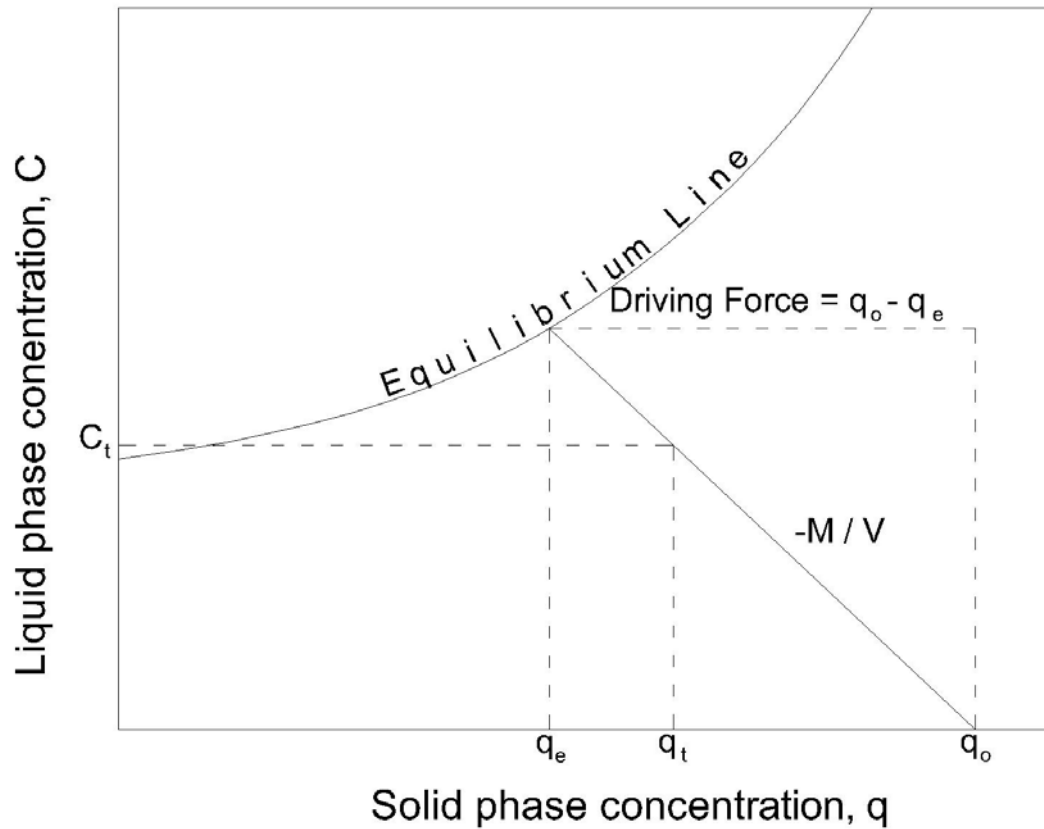


Figure 2-8 Operating diagram of a desorption process from a resin with an initial concentration q_0 .

As seen in the diagram a given amount of resin and volume of solution determine the slope of the operating line ($-M/V$); the driving force is represented by the difference between q_0 and q_e .

In this work, the adsorption and desorption of perchlorate onto a highly selective IX resin was studied. The equilibrium, kinetics and biological regeneration behavior were examined by carrying out a number of experiments contacting the resin with perchlorate solutions for adsorption and equilibrium, with 6% NaCl solution for desorption and with a perchlorate-reducing culture for the biological regeneration. The data collected was then analyzed using different models presented in the literature to gain better understanding of the mass transport and biological degradation of perchlorate from the resin.

CHAPTER 3 MATERIALS AND METHODS

3.1 Resin Conditioning

This research was performed using an ion exchange resin commercially available as a highly perchlorate selective product. This resin is classified as a macroporous styrene SBA resin with N-tributyl amine functional group as shown in Figure 3-1.

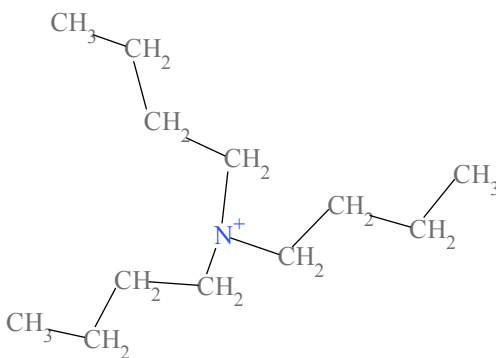


Figure 3-1 N-butyl amine functional group of the studied resin.

The resin was conditioned following the procedure of Tripp (2001). Approximately 100 mL of resin was placed in a 1 inch (i.d.) glass column. The resin was rinsed with deionized water for 2 hours at a flow of 10 mL/min. The resin was then exposed to acid-base cycling by pumping a 1 N solution of sodium hydroxide down-flow for at least one hour at a flow rate of 8 mL/min in order to convert the resin to the hydroxide form.

The resin was then rinsed with at least 10 bed volumes of deionized water down-flow through the resin bed at a flow rate of 8 mL/min. The rinsing was then followed by a conversion of the resin to the chloride form by pumping a 1 N solution of hydrochloric

acid at a flow rate of 8 mL/min down flow through the resin bed for at least one hour. The resin in the chloride form was then rinsed with at least 10 bed volumes of the deionized water at a flow rate of 8 mL/min down-flow, completing the first acid-base cycle. This procedure was repeated for two more cycles. For the final rinsing with deionized water the pH of the effluent water was measured and the rinsing was stopped when a stable pH endpoint was reached. The resin in the chloride form was then transferred to a beaker and placed to dry at 40°C for 24 hours. The resin in the beaker was then air-dried and equilibrated for seven days at room temperature. After this, the beaker was covered with Saran® wrap and stored until needed.

3.2 Column Resin Exhaustion

A column exhaustion test was carried out by placing 0.5 g of conditioned resin into a 10 mm diameter column. The column was then filled with deionized water and it was left for 24 hours to allow the resin to expand. A previous study by Hiremath et al. (2006) used culture NP30 and showed the reduction of perchlorate from water samples from La Puente below detection limits. Based on this results a concentrated solution with similar ratio of ions as in water from La Puente Valley County Water District in California (Table 3-1) was prepared. In order to accelerate the exhaustion process the prepared solution concentration was 200 times the La Puente composition. All salts used were reagent grade in the sodium form.

Table 3-1 La Puente concentration of ions.

Property	Units	Value
Total alkalinity	mg CaCO ₃ ⁻ / L	181
Conductivity	μS	491
ClO ₄ ⁻	μg/L	54
NO ₃ ⁻ as N	mg/L	5.7
SO ₄ ⁻	mg/L	31

The column was operated at a flow rate of 2 mL/min (0.75 empty bed contact time, EBCT). Samples of the effluent were collected at given time intervals and analyzed for ClO₄⁻ concentration as described in the analytical techniques section. Each collected sample was equal to 6 minutes (12 mL) of effluent composition.

A simulation program of the column effluent histories was used to compare with the experimental results. The program was developed at the University of Houston based on Equilibrium Multicomponent Chromatography Theory (EMCT-Windows 2.0). Input of the composition of the feed water, separation factors of the components and resin capacity provides an output of the effluent concentration versus BV. The input data used in the program is presented in Table 3-2.

Table 3-2 Input data for EMCT simulation.

Property	
Resin capacity (meq/L)	0.5
Bed porosity	0.4
Separation factor	
ClO_4^-	1
NO_3^-	6
SO_4^-	11
HCO_3^-	100
Cl^-	4700

The perchlorate/chloride separation factor used was determined experimentally as described in section 3.4, the other separation factors used were the ones provided by the EMCT program.

3.3 Sorption Isotherms

Batch experiments were conducted to determine sorption isotherms. For these experiments serum bottles were filled with varying masses of conditioned resin and a 100 mL solution with a total anionic concentration of 5 meq/L as shown in Figure 3-2. The solution was prepared using 0.005 meq/L (0.5 mg/L) of perchlorate and 4.995 meq/L (177 mg/L) of chloride to resemble the La Puente concentration of ions but replacing all ions except perchlorate with chloride.



Figure 3-2 Serum bottles with resin in 100 mL solution for sorption isotherm test.

The bottles were set on a rotary shaker at 120 rpm and samples of the solution were taken after 24 hours and 168 hours (1 week) of equilibration. The perchlorate concentration in the sample was determined by ion chromatography as described in the analytical techniques section.

3.4 Separation Factor

In order to estimate the perchlorate/chloride separation factor, tests were performed in a similar fashion as that for the sorption isotherms described above. The solution initial concentration of perchlorate was 5.6 mg/L in a 6% NaCl brine. Samples gathered after 1 week of equilibration were prepared and analyzed using ion chromatography. Mass balances were calculated to determine the average separation factor.

3.5 Sorption Kinetics

For the kinetic studies 1.0 g, 2.0 g and 3.0 g of conditioned resin were weighed and placed inside an Erlenmeyer containing 1 L of Type I water with a 1000 mg/L perchlorate concentration. The test was carried out at 20 °C and was mixed in a shaker at 125 rpm. Samples were taken at given time intervals by stopping the stirring to let the resin settle. A 5 mL sample of the supernatant was taken and diluted with deionized water. Then the perchlorate concentration was measured with a perchlorate ion-selective electrode as described in the analytical section. The electrode was used when perchlorate concentration was higher than 1 mg/L.

The same procedure was followed after weighting 1.0 g, 2.0 g and 3.0 g of conditioned resin that was placed inside a membrane Spectrum Spectra/Por® 6 RC dialysis membrane tubing 50,000 Dalton molecular weight cut-off (MWCO). The membrane was closed with a clamp at one end and a magnetic closure at the other end and placed inside an Erlenmeyer containing 1 L of solution with a 1000 mg/L perchlorate concentration as shown in Figure 3-3.

Once the adsorption experiments were completed, the solution was discarded; the resin was rinsed with 5 mL of ethanol and then rinsed with 600 mL of deionized water. The resin was then transferred to a smaller container with deionized water and kept in the refrigerator waiting for desorption tests.



Figure 3-3 Set up for kinetics adsorption experiments of resin inside the membrane.

For the desorption tests, the loose resin and the resin inside the membrane were placed in an Erlenmeyer with 200 mL of 6% NaCl solution. Each Erlenmeyer was placed on top of a magnetic stirrer and 5 mL samples of each were collected at given time intervals. The perchlorate concentration was measured with the perchlorate ion-selective electrode as described in the analytical section.

3.6 Biological Regeneration of Exhausted Resin

3.6.1 Resin Exhaustion

Prior to biological regeneration, the resin was exhausted by preparing eight serum bottles each with 1.0 g of air-dried resin in 150 mL of 1,122 mg/L of perchlorate dissolved in Type I water. The bottles were set in a shaker table at 110 rpm and 20°C for one week after which a sample from the supernatant was taken and the perchlorate concentration was measured using a perchlorate selective electrode as described in the analytical section. Then the solution was discarded and 5 mL of ethanol were added to each bottle followed with a rinse with 600 mL of deionized water. The exhausted resin was then transferred into a membrane and clamped at each end.

3.6.2 Media Preparation

A synthetic medium was prepared for development and maintenance of culture NP30. The composition of the synthetic medium presented in Table 3-3, was based on the general marine medium composition with trace metal added as developed by Cang et al. (2004). Sulfate was omitted to avoid the development of sulfate-reducing bacteria. Sodium acetate was used as sole electron donor and perchlorate desorbing from the resin acted as electron acceptor.

Table 3-3 Composition of 6% synthetic medium prepared for culture NP30.

Component	Concentration
MgCl₂·6H₂O	0.1 mol/mol to Na
NaCl	6%
CH ₃ COONa·3H ₂ O	1.23 g/L
NaHCO ₃	200 mg/L
CaCl ₂ ·2H ₂ O	1.4 g/L
KCl	0.72 g/L
KH ₂ PO ₃	75 mg/L
Mineral solution	1.0 mL/L
Mineral solution (g/L):	
(NH ₄) ₆ Mo ₇ O ₂₄ ·H ₂ O	10
ZnCl ₂	0.05
H ₃ BO ₃	0.3
FeCl ₂ ·4H ₂ O	1.5
CoCl ₂ ·6H ₂ O	10
MnCl ₂ ·6H ₂ O	0.03
NiCl ₂ ·6H ₂ O	0.03

As established in a previous study by Lin (2007) the Mg/Na ratio of 0.11 was maintained for optimal conditions. During the preparation of the medium, anaerobic culture techniques were followed (Hungate, 1969). The synthetic medium was boiled on a hot plate for 2 minutes in order to remove dissolved oxygen and then cooled under a flush of nitrogen gas in an ice bath.

3.6.3 Inoculum Source

The inoculum was obtained from the salt-tolerant perchlorate-degrading culture developed by Cang et al., 2004. Since the parent culture is maintained in a 3% synthetic media containing perchlorate, the biomass drawn for the experiments was centrifuged at

1,000 rpm for 2 minutes and washed twice with 6% synthetic media to remove any residual perchlorate, and then it was resuspended in synthetic medium. A sample was then taken to establish the volatile suspended solids (VSS) concentration.

3.6.4 Biological Regeneration of Exhausted Resin

Each one of the perchlorate exhausted resins inside the membranes was placed in a 250 mL Erlenmeyer that was previously flushed with oxygen-free nitrogen gas for 2 minutes. Then 3 mL of culture NP30 and 200 mL of medium were added to each one of the tests, the air was displaced with nitrogen and then the Erlenmeyer was sealed with a rubber stopper incorporated with a short piece of plastic tubing protruding from the top and clamped to avoid air entering the test. Each test was then placed on a magnetic stirring plate. At time intervals each test was sampled by inserting a syringe into the tubing and connecting it to the attachment on the tubing. Then the clamp was removed and approximately 1 mL of the solution was sampled. Then the tubing was clamped back and the syringe removed.

The content of the syringe was placed in a labeled snap-cap microcentrifuge tube. All the samples were centrifuged at 14,000 rpm for 2 minutes to separate the biomass. Then 0.8 mL of the supernatant was taken and diluted in 8 mL of DI water. These diluted samples were analyzed for ClO_4^- concentration as described in the analytical methods section.

3.7 Analytical Methods

3.7.1 Ion Chromatography

When the perchlorate concentrations were less than 1 mg/L, they were determined using a Dionex ICS-3000 Ion Chromatography system (Dionex, Corp, Sunnyvalley, CA) conforming with the US EPA Method 314.2 (2008) with minor modifications for applications in high salt samples. The system is comprised of a Dual Pump (DP) module, Eluent Generator (EG) module, Detector/Chromatography (DC) module and AS Autosampler with a 5 mL loop, 8.2 mL sampling needle assembly, two EluGen EC II NaOH cartridges, two Continuously Regenerated Anion Trap Columns CR-ATC, four 4 L plastic bottle assemblies for external water use operation, Chromeleon Chromatographic Workstation, Dionex IonPac AG16 and AS16 2 mm columns, a ASRS ULTRA II (2mm) suppressor.

3.7.2 Perchlorate Probe

For perchlorate concentration above 1 mg/L, a Thermo Scientific Orion 93 series perchlorate module was used with a Thermo Scientific Orion ISE meter (Thermo Fisher Scientific Inc., Beverly, MA). The specifications included a concentration range 0.70 to 99,500 ppm, pH range of 2.5 to 11, electrode resistance of 1 to 5 megaohms and $\pm 2\%$ reproducibility. The electrode was calibrated with standard perchlorate solutions and a standard curve was prepared of the log of the concentration versus the potential (mV) as shown in Appendix B.

Samples were diluted by using 0.2 mL of sample in 1.8 mL of DI water, the tip of the electrode was inserted in the solution and the electrode potential reading was recorded and converted to concentration of perchlorate in mg/L.

CHAPTER 4 RESULTS

Developing a process for the biological regeneration of a perchlorate exhausted SBA resin requires a thorough understanding of the characteristics of the resin behavior during the process of adsorption and desorption. The analysis of the results included estimating the resin capacity and breakthrough, the equilibrium behavior and the kinetics and controlling mechanisms of perchlorate adsorption and desorption. The gathered information was then applied to the biological regeneration of the resin in indirect contact with the culture NP30.

4.1 Resin Capacity

Column experiments were conducted prior to batch experiments in order to observe resin performance and determine resin capacity and breakthrough. The influent solution was a composite prepared with the ions present in concentrations resembling water from La Puente in California and presented in Table 3-1 with a flow rate of 2 mL/min (0.75 empty bed contact time, EBCT). Samples of the effluent were collected at time intervals and analyzed for ClO_4^- concentration. The resin is considered exhausted at breakthrough which is observed when ClO_4^- appears in the effluent because of the lack of available sites for ion exchange.

The results from the column exhaustion test are shown in Figure 4-1 as the ratio of perchlorate concentration in the effluent to initial concentration versus bed volumes (BV). Breakthrough of ClO_4^- occurred after approximately 5700 BV. Under the

experimental conditions a 10% breakthrough would still be under the treatment target of 6 ppb.

The resin operating capacity can be estimated from the breakthrough curve by means of calculating the area above the curve and knowing the mass of resin loaded. Following this procedure it was estimated this resin had an operating capacity of 1.1 meq/g of dry resin.

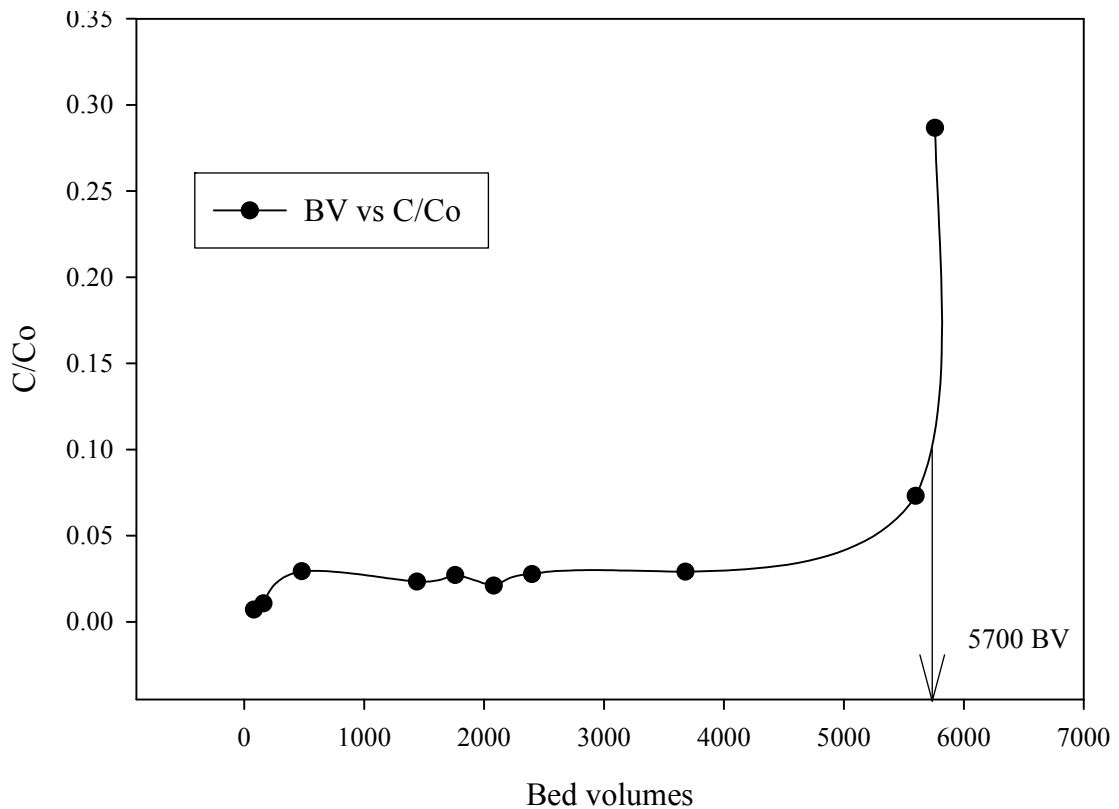


Figure 4-1 Column exhaustion breakthrough of ClO_4^- for La Puente water composition, 2 mL/min flow rate and 20°C.

In addition to the column study, a batch experiment consisting of 0.53 g of dry resin added to 100 mL solution of 700 mg/L of perchlorate was performed. The bottle was mixed on a rotary shaker at 120 rpm and samples were taken at 0, 5, 15, 30, 60 and 120 minutes and at 24 hours. After 24 hours 99.995% of the perchlorate had been adsorbed. From a mass balance the capacity of the resin was determined to be 1.4 meq/g of dry resin. The manufacturer provided a specification of wet volume capacity of the resin in the chloride form of 0.60 meq/mL of resin. The measured resin volume to mass ratio was 3.11 mL/g so the calculated capacity is 1.9 meq/g. Based on these results the average capacity of the resin was 1.45 meq/g. Table 4-1 presents a summary of some properties of commercially available SBA resins used in published studies dealing with perchlorate adsorption. The capacity results obtained by this work are comparable to those published by other studies.

Table 4-1 Capacities of commercial perchlorate selective IX resins.

Resin name	Matrix	Functional Group	Capacity meq/mL	Ref.
This work	STY-DVB	Tributylamine	0.5	This work
SIR-110	STY-DVB	Tributylamine	0.6	Hristovski et al., 2008
A530E	STY-DVB	Triethylamine	0.55	Xiong et al., 2007
IRA 958	Polyacrylic	Trimethylamine	0.75	Tripp 2001
IRA 900	STY-DVB	Trimethylamine	1.05	Tripp 2001
CalRes 2103	STY-DVB	Quaternaryamine	1.4	Hristovski et al., 2008
Amberlite PWA2	STY-DVB	N/A	0.6	Hristovski et al., 2007

The software application called EMCT 2.0 developed at the University of Houston was used to simulate the column experiment. The program calculates the breakthrough

time for several components based on separation factors and influent concentrations supplied by the user. The results from the simulations are presented in Table 4-2 and predicted breakthrough at 5758 bed volumes which closely match the experimental results shown in Figure 4-1.

Table 4-2 EMCT predicted results.

BV	ClO_4^- mg/L	NO_3^- mg/L	SO_4^{2-} mg/L	HCO_3^- mg/L	Cl^- mg/L
					3.704
162					3.704
162				3.704	
572				3.704	
572			0.721	2.983	
965			0.721	2.983	
965		0.092	0.646	2.967	
5758		0.092	0.646	2.967	
5758	5.43E-04	0.092	0.645	2.966	
6000	5.43E-04	0.092	0.645	2.966	

* The results represent the concentration of the ion in the column effluent

4.2 Equilibrium Studies

An understanding of equilibrium is required to design a reactor for the biological regeneration of the exhausted resin. Sorption equilibrium isotherm and separation factors describe equilibrium. Equilibrium isotherm experiments were carried out, the results were analyzed using Freundlich and Langmuir models, and the mass balances were calculated to determine the separation factor.

Figure 4-2 and Figure 4-3 present the Freundlich and Langmuir experimental data and the results the plots of the fitted lines with the regression coefficients.

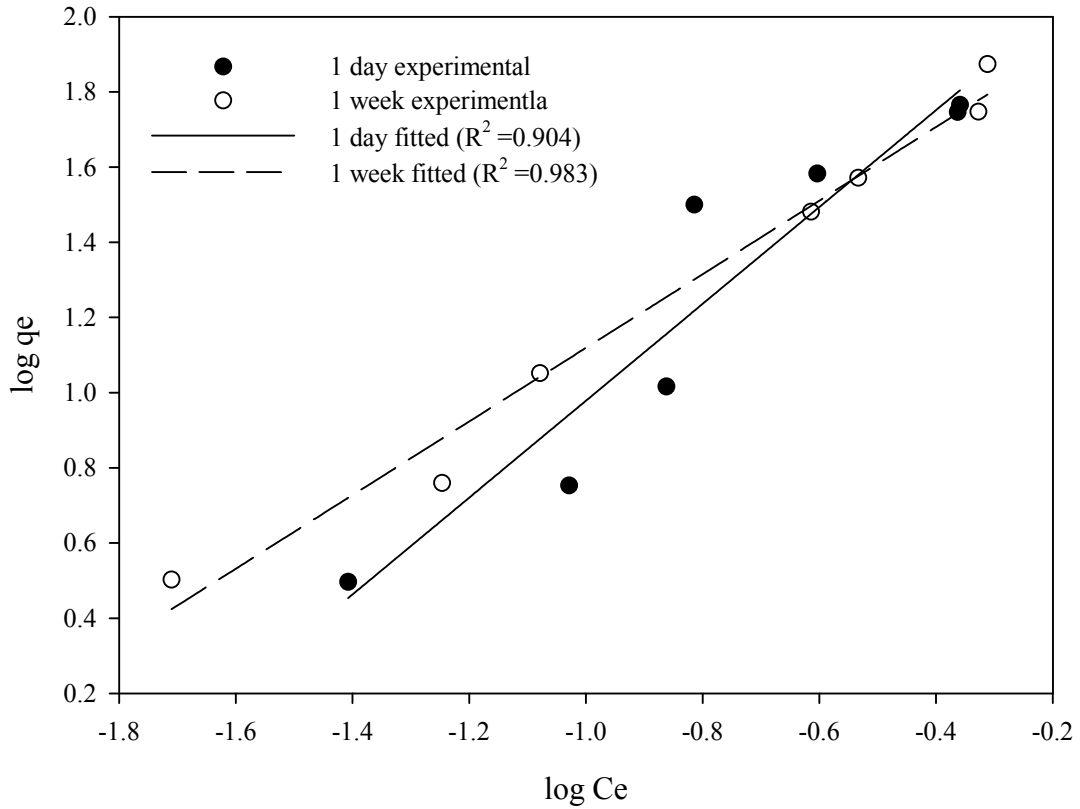


Figure 4-2 Freundlich isotherms for samples equilibrated during 1 day and 1 week at 20°C.

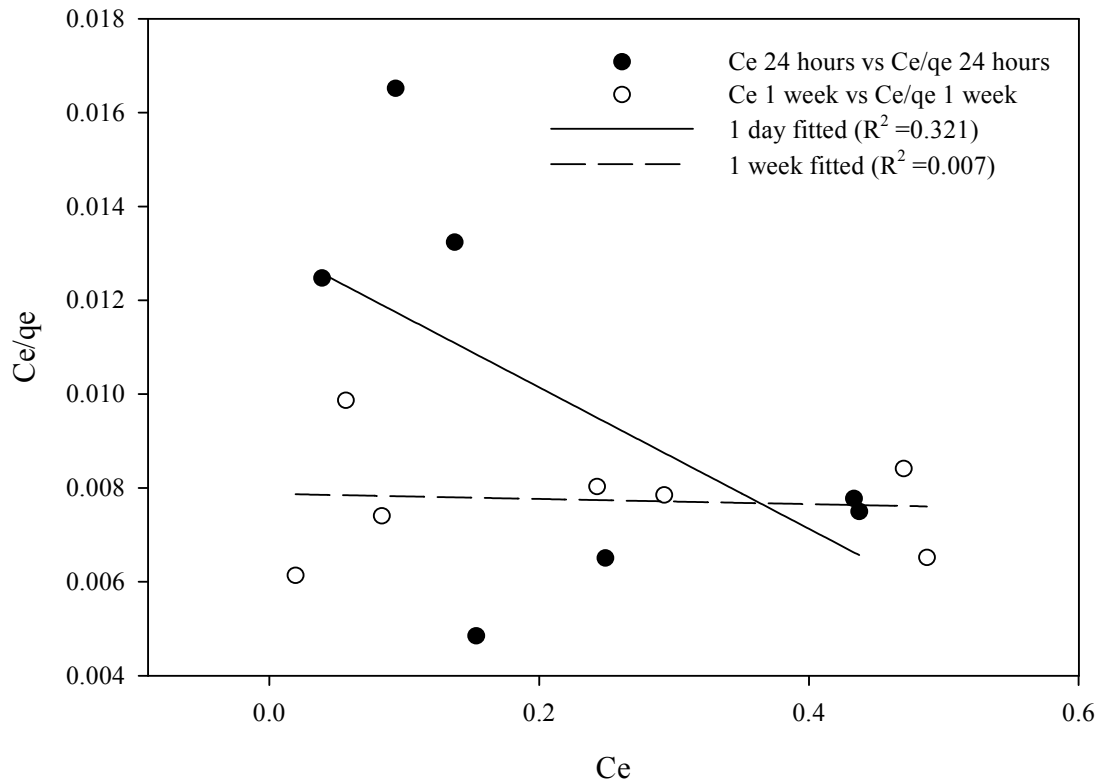


Figure 4-3 Langmuir isotherms for samples equilibrated during 1 day and 1 week at 20°C.

A better fit to the data was obtained using the Freundlich isotherm model presented in equation 4-1:

$$q_e = K_F C_e^{1/n}, \quad 4-1$$

where:

K_F is the Freundlich adsorption capacity parameter $(\text{mg/g})(\text{L/mg})^{1/n}$,

$1/n$ is the Freundlich adsorption intensity parameter, unitless.

The Freundlich equation applies to non-ideal sorption on a heterogeneous or multilayer surface. A value of $n > 1$ represents favorable adsorption conditions (MWH, 2005; Abdullah, 2009).

Perchlorate concentrations in solution and in the resin phase of equilibrated samples at 24 hours and one week were plotted using the Freundlich model as shown in Figure 4-4. The linear regression and the 95% interval of confidence levels (dashed lines) show the comparability between data for 24 hours and one week. Consequent equilibrium studies were performed considering that equilibrium was reached by 1 week.

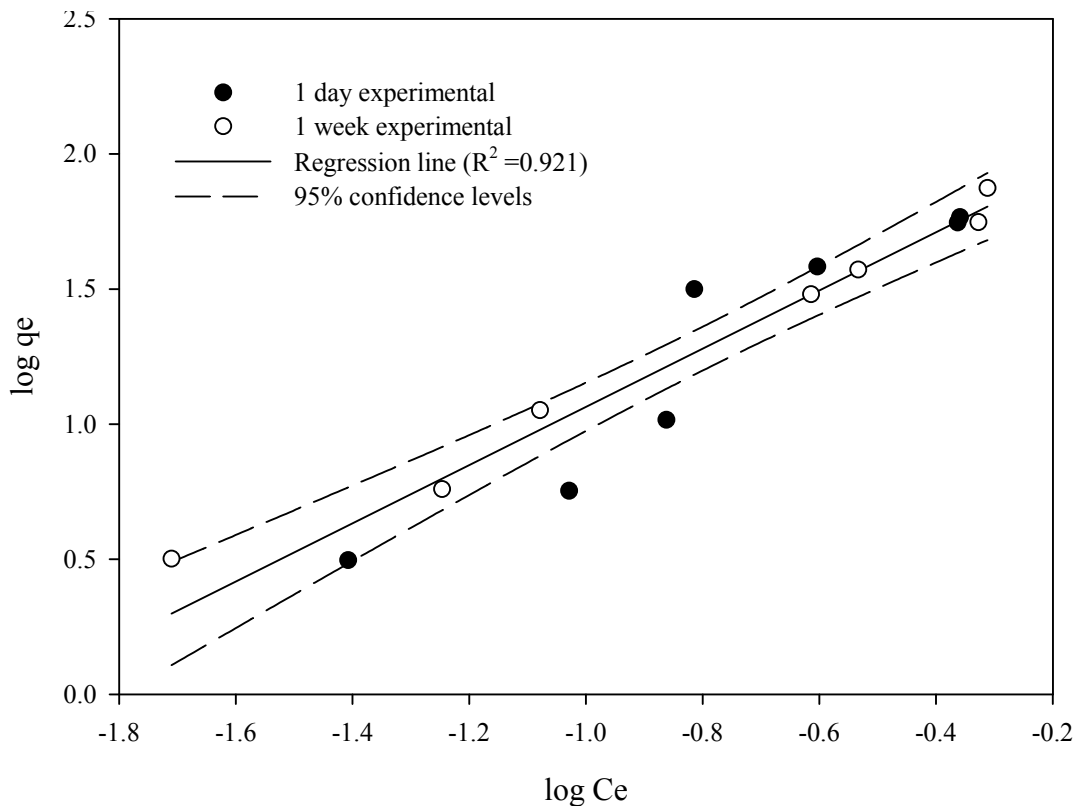


Figure 4-4 Comparison of 24 hours and one week equilibrium sorption isotherms. Samples taken at 20°C.

A second set of isotherm experiments was performed using a wider range of resin masses. The reversibility of perchlorate adsorption of this samples, was tested by rinsing the equilibrated resin to remove the isotherm solution after adsorption and then placing it in a 6% NaCl solution to initiate desorption until equilibrium was reached. Figure 4-5 presents a comparison of the results for the adsorption and desorption isotherms. The plotted line shows a linear regression and the dashed curves present the 95% confidence interval of the prediction. The correlation coefficient was 0.879 indicating that the adsorption and desorption equilibrium are reproducible.

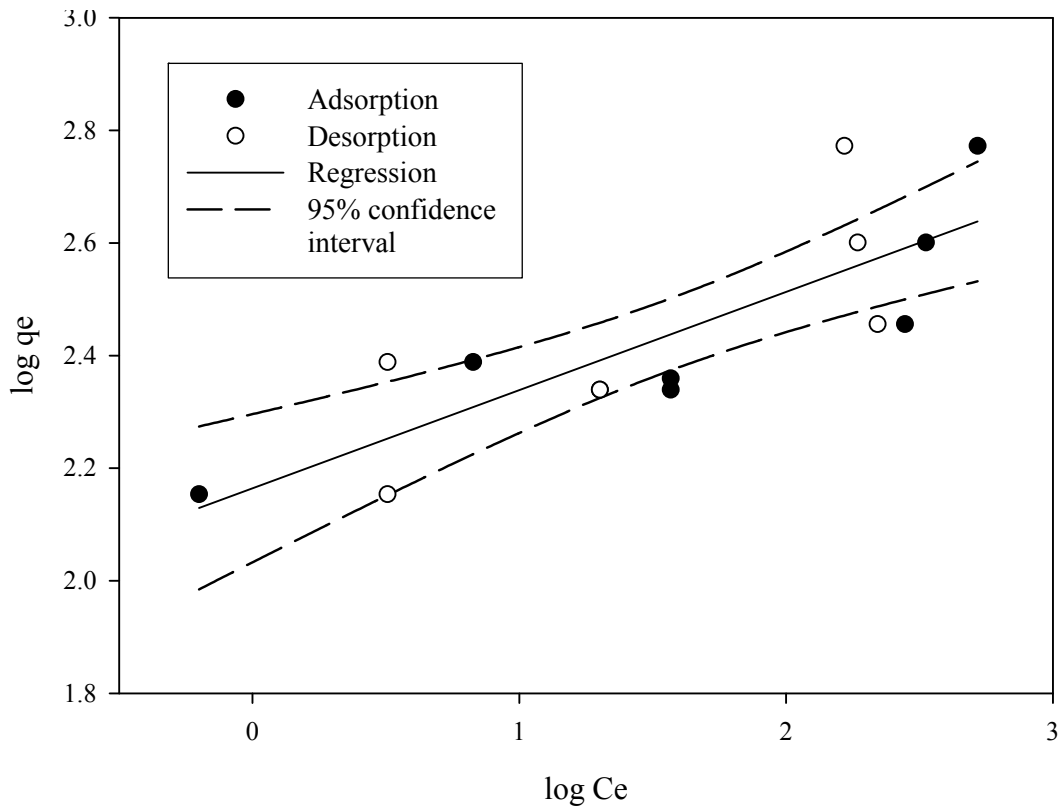


Figure 4-5 Adsorption and desorption isotherm for samples taken at 20°C after 24 hours of equilibration. Desorption on 6% NaCl.

Figure 4-6 presents the results including those used in Figure 4-4 and Figure 4-5, plotted using the Freundlich model. The averaged data from the 24 hours and one week and adsorption and desorption results for each resin amount was used in the plot.

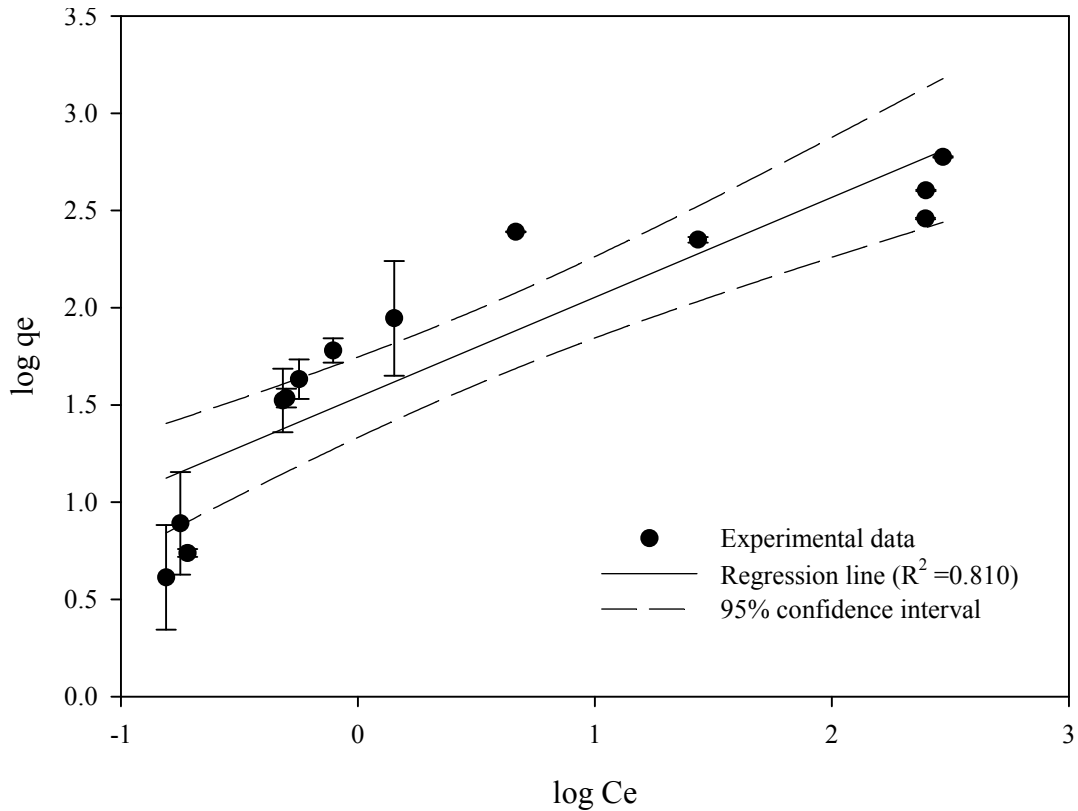


Figure 4-6 Freundlich equilibrium sorption isotherms at 20°C. Data averaged for 24 hours and 1 week, adsorption and desorption for each mass of resin tested.

A study by Yoon et al., 2008 on perchlorate sorption onto resin SR-7 also found that the Freundlich model provided the best fit for the experimental data. Similarly, a paper by Xiong et al., 2007 reported the results of perchlorate sorption isotherms on several classes of IX resins that were also described best by Freundlich model. Table 4-3 summarizes these results for the SBA resin tested.

Table 4-3 Freundlich model parameters of SBA resins.

Resin name	Matrix	Functional Group	Freundlich coefficients and correlation			Ref.
			K_F	n	R^2	
This work	STY-DVB	Trybutylamine	50	2.36	0.83	This work
SR-7	STY-DVB	Tripropylamine	12.6	2	NR	Yoon et al., 2009
A-530	STY-DVB	Triethylamine	91	3.45	0.91	Xiong et al., 2007
IRA 900	STY-DVB	Trimethylamine	25	2.04	0.97	Xiong et al., 2007
IRA 958	Polyacrylic	Triethylamine	5	3.22	0.95	Xiong et al., 2007

NR = not reported

The results of the Freundlich coefficients are comparable with those determined for SBA resins in similar studies. All styrene resins have higher values of K_F than the acrylic resin, and are within the same order of magnitude.

4.2.1 Separation Factor

Perchlorate-chloride separation factors for each test performed were calculated from equations 2-4 to 2-8 and the mass balance equations are presented below:

$$Y_{ClO_4^-} = \frac{(C_i - C_e) \times V}{Q_T \times g}, \quad 4-2$$

$$Y_{Cl^-} = 1 - Y_{ClO_4^-}, \quad 4-3$$

where:

C_i is the initial perchlorate concentration (meq/L),

V is the solution volume (L),

g is the dry mass of resin (g).

The calculated average perchlorate-chloride separation factor was 4700 ± 1700 . This result was used in the EMCT calculation of the effluent histories for the column exhaustion process.

The high separation factor is a consequence of several characteristics of the resin. It has been shown that polystyrenic resins have higher separation factors than polyacrylic resins. Also that as the length of the alkyl group bonded to the quaternary amine increases the separation factor increases, from 125, 1100 and 1500 for methyl to ethyl to propyl respectively (Tripp, 2001), and now 4700 for butyl from this study. It has also been observed that the longer the chain the slower the kinetics (Batista et al., 2002) which explains why the studied resin is used as a single use resin for removal of perchlorate from drinking water. Regenerating this resin would be kinetically unfavorable and would require a vast amount of highly concentrated sodium chloride (6 to 12 percent).

4.3 Kinetic Studies

Kinetic studies are imperative for designing a reactor for the biological regeneration of perchlorate exhausted resins. These studies provide information on the adsorption and desorption rate processes, mass transfer control mechanism, and diffusion and mass transfer constants which are important in determining flow rates, reactor size and configuration.

Xiao et al. (2010) demonstrated the biological regeneration of perchlorate exhausted resins with the culture NP30 in direct contact with the resin. But there is apprehension in the drinking water industry to reusing this regenerated resin unless it is cleaned and sterilized. A regeneration process in which the resin is not in direct contact with the culture is proposed by means of placing the resin inside a dialysis membrane tube (50,000 MWCO). Adsorption and desorption experiments were conducted with the resin loose and inside the membrane and the following sections discuss the results.

4.3.1 Adsorption Studies

Results from the adsorption experiments performed using 1.00, 2.00 and 3.00 g of loose resin and the same amounts of resin inside the membrane are shown in Figure 4-7. The graph depicts the first 60 minutes of data of perchlorate concentration in the solution related to the initial concentration (C/C_0) versus time in minutes.

There is an effect of resin mass on perchlorate adsorption on the loose resin. The amount of perchlorate adsorbed during the first 60 minutes shows that as the resin mass increases the amount of adsorbed perchlorate increases. On the other hand, for the resins contained inside the membrane the adsorbed amount of perchlorate after 60 minutes is very similar regardless of the mass.

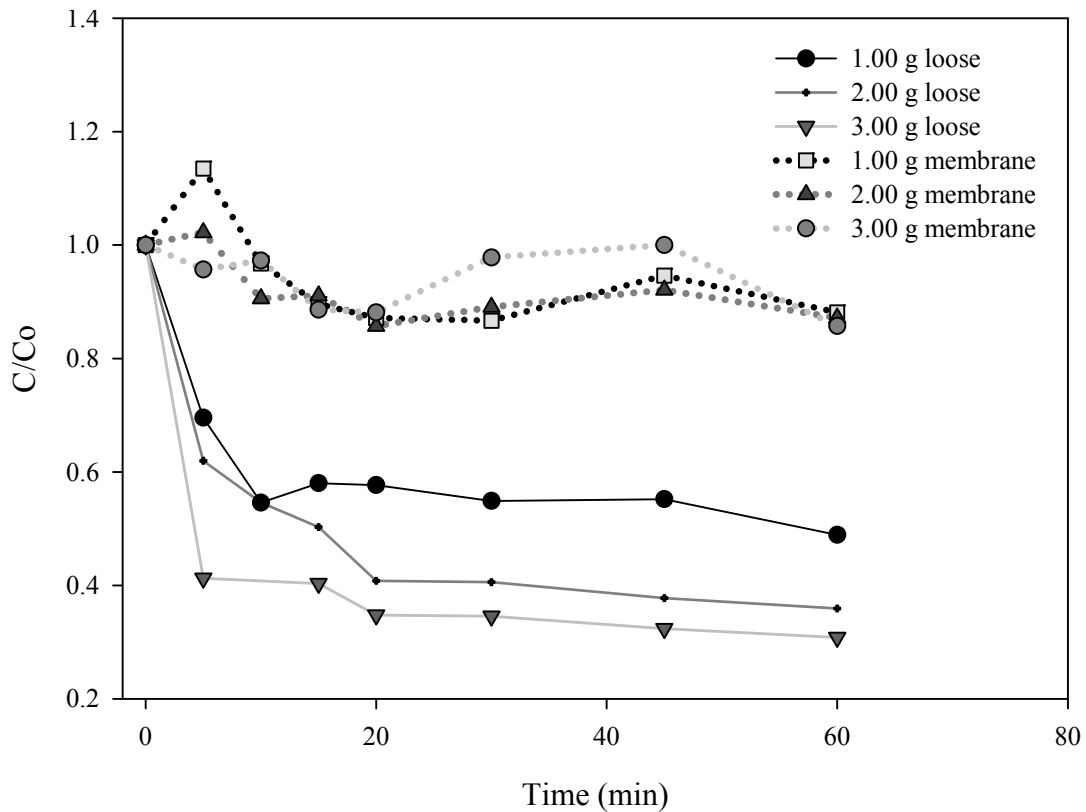


Figure 4-7 Comparison of sorption kinetics resin loose and inside membrane data presented for 60 minutes at 20°C.

As was expected, the loose resin adsorption rate and total capacity is higher than the adsorption rate for the resin inside the membrane. This can be explained in terms of the mass transfer process, the loose resin is in direct contact with the solution and is being mixed vigorously, which enhances the rate of mass transfer by eliminating the resistance to mass transfer from the liquid film around the particle. Although the membrane-resin set is being stirred, the resin inside the membrane is not subject to the same amount of agitation.

Figure 4-8 shows the results of the same adsorption experiment but data for up to 72 hours is presented.

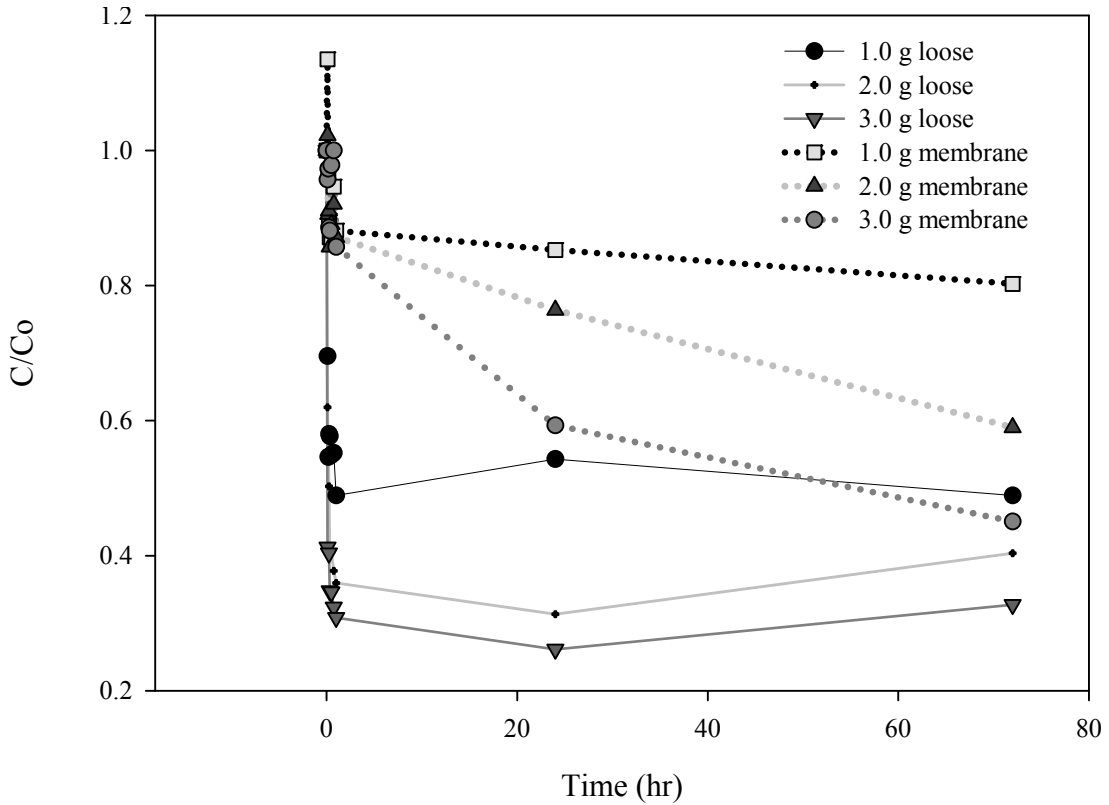


Figure 4-8 Comparison adsorption kinetics loose resin and in membrane data presented for 72 hours at 20°C.

Perchlorate adsorption on the loose resin approaches a similar saturation of C/C_0 after 72 hours. In contrast the resin inside the membrane shows that as the mass of resin increases the amount and rate of adsorption of perchlorate on the resin also increases. On the other hand, the adsorption rate of the loose resin is approaching zero compared to the adsorption rate of the resin in the membrane after the initial 60 minutes of adsorption because the equilibrium had been reached.

In conclusion the loose resin reaches equilibrium very fast, within the first hour as opposed to the resin inside the membrane which takes a long time to reach equilibrium. The mass transfer in the loose resin is subject to the convection from the bulk of the liquid to the resin surface and then the diffusion process that happens in the resin surface and pores. The mass transfer in the resin inside the membrane has an additional resistance given by the liquid film on the surface of the particle.

4.3.2 Desorption Studies

After the adsorption experiments were completed, the resin was rinsed and prepared for desorption in a 6 % NaCl brine. The figures below show the results for 2.00 and 3.00 g of resin. Figure 4-9 presents a comparison of the adsorption and desorption of perchlorate for the resin that was loose, C_0 is the initial perchlorate concentration in the adsorption experiments. Both sorption processes reach equilibrium within the first hour. The mass transfer rate is high and this observation applies for both masses of resin. During the adsorption around 80% of the initial amount of perchlorate was exchanged while only 20% was desorbed after 72 hours. The resin studied is not only highly selective but also binds perchlorate tightly making it a non-regenerable SBA resin.

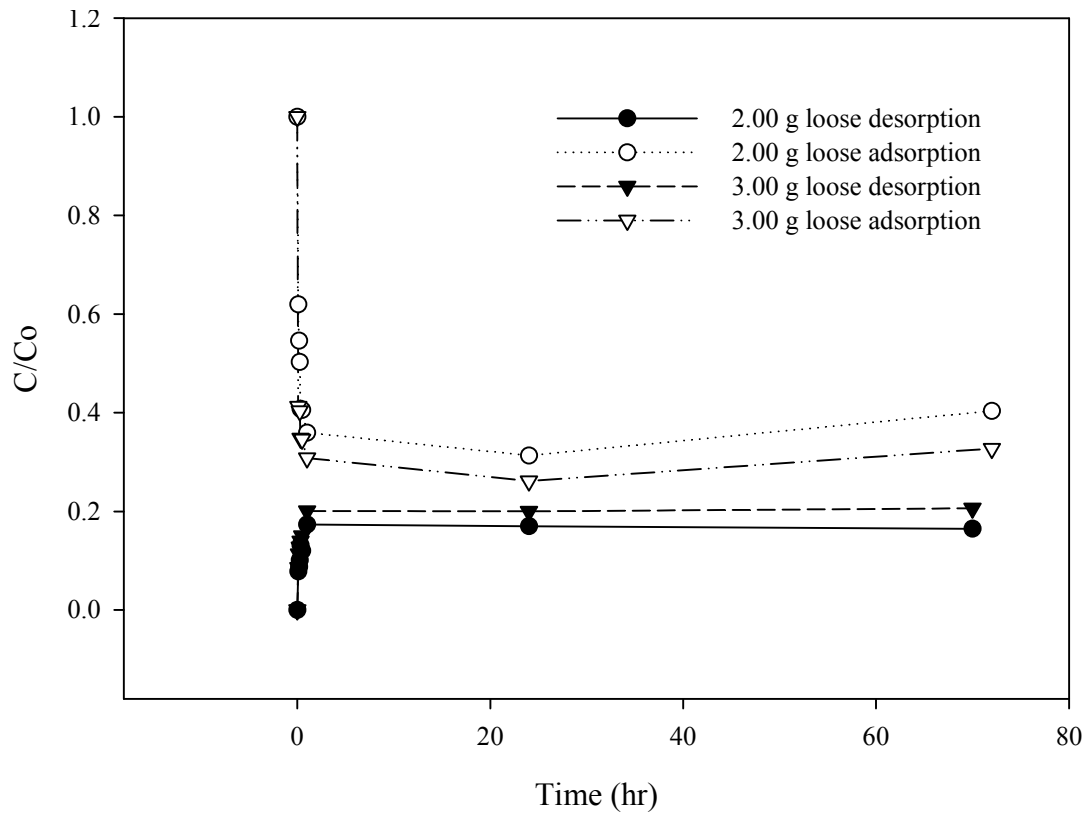


Figure 4-9 Comparison of adsorption and desorption of perchlorate on 2.00 and 3.00 g of loose resin at 20°C. C_0 is initial perchlorate concentration of adsorption experiment.

The same type of comparison is represented on Figure 4-10 for the resin inside the membrane. In this case the mass transfer rate is low and more time is required to reach equilibrium for both sorption processes. The resin desorbed around 20% of the initial amount of perchlorate after 72 hours, which is similar to the ultimate desorbed amount from the loose resin.

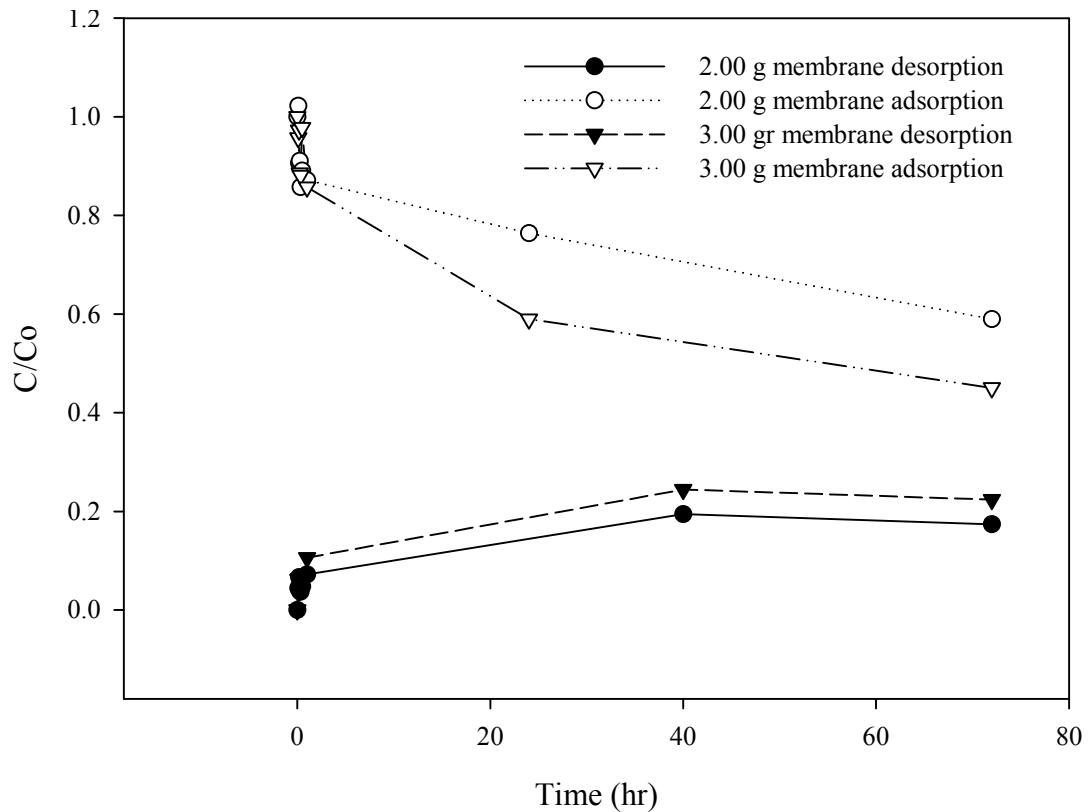


Figure 4-10 Comparison of adsorption and desorption of perchlorate on 2.00 and 3.00 g of resin inside the membrane at 20°C. C_0 is the initial perchlorate concentration of the adsorption experiments.

It is important to point out that desorption results show that perchlorate concentration reaches equilibrium at around 20% of the initial concentration. This is true in both of the studied arrangements: loose and membrane. Moreover, this is also true for both resin amounts in the membrane experiment as presented in Figure 4-11. This suggests that the mass transfer process for desorption is independent of these two factors and it is a function of the of resin characteristics such as matrix type and functional groups.

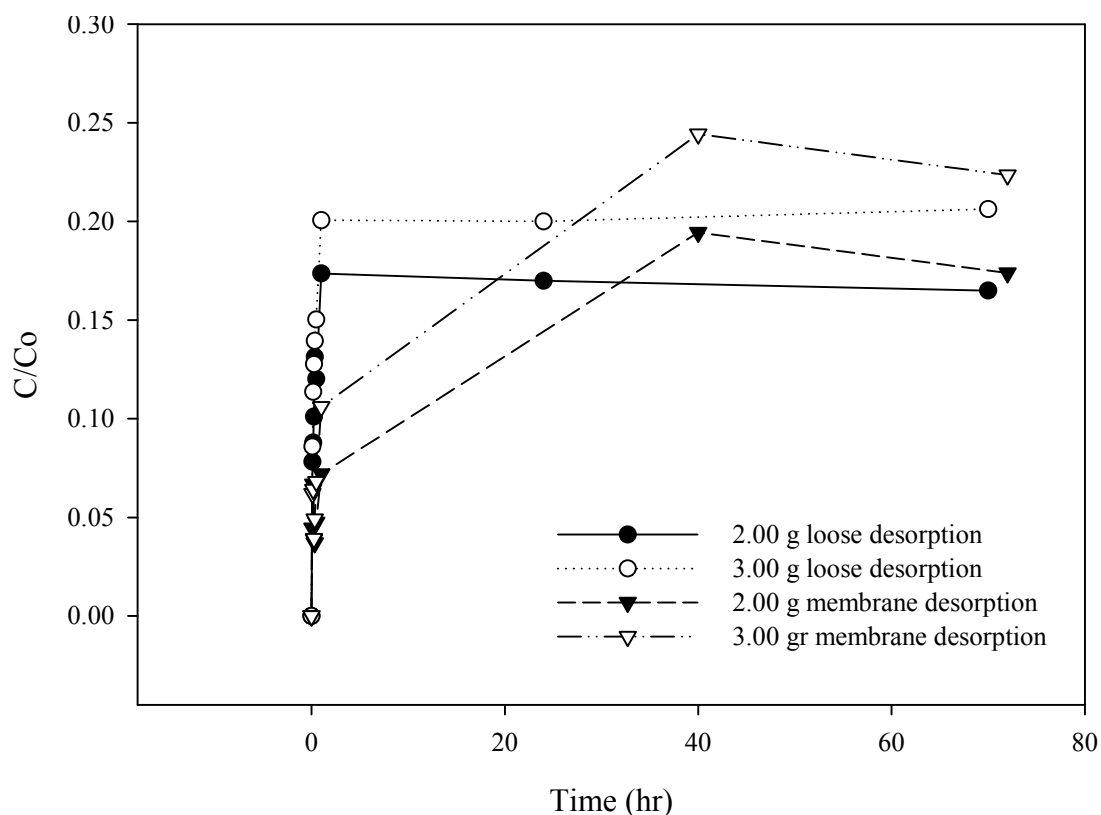


Figure 4-11 Comparison of adsorption and desorption of perchlorate on 2.00 and 3.00 g of resin loose and inside the membrane at 20°C.

The sorption experiments provided valuable information about the mass transfer mechanisms that take place during the adsorption and desorption of perchlorate. The results show that perchlorate tightly binds to the studied resin. For this study it was proposed to regenerate the resin using a salt-tolerant perchlorate-reducing culture separated from the resin by the membrane. The idea was to avoid reaching equilibrium by constantly degrading the desorbed perchlorate thus maintaining a delta in the perchlorate concentration that would allow for more perchlorate to be desorbed from the resin.

4.4 Mass Transport and Diffusion

4.4.1 Diffusion Controlled Sorption Studies

One of the main objectives of this work was to determine the controlling mechanism of mass transfer. During sorption there is a transport process governed by one or more of the following processes: convection from the bulk of the liquid to the liquid film on the resin's surface, external mass transfer through the liquid film, diffusion taking place inside the resin pores and adsorption onto the resin surface by ion exchange reaction. Figure 2-7 presented in the literature review chapter shows a depiction of these processes.

In the experiments with the loose resin it was assumed that the convection and liquid film resistances were minimal due to the agitation. In this case diffusion and/or adsorption become the controlling factors for perchlorate transport from the bulk of the liquid into the resin pores and adsorption into the resin. Assuming that the adsorption takes place fast, then the diffusion coefficient can be determined from the loose resin experimental results. Under these conditions the process can be described by applying Equation 2-8 which is the intraparticle diffusion equation. The methodology used consisted of preparing a plot of the adsorption/desorption kinetics experimental data from the loose resin experiments and a plot of data from the analytical solution to the governing differential equation. The differential equation was solved by trial and error of the diffusion coefficient until the resulting plot replicated the experimental data. The results are presented in Figures 4-12, 4-13 and 4-14.

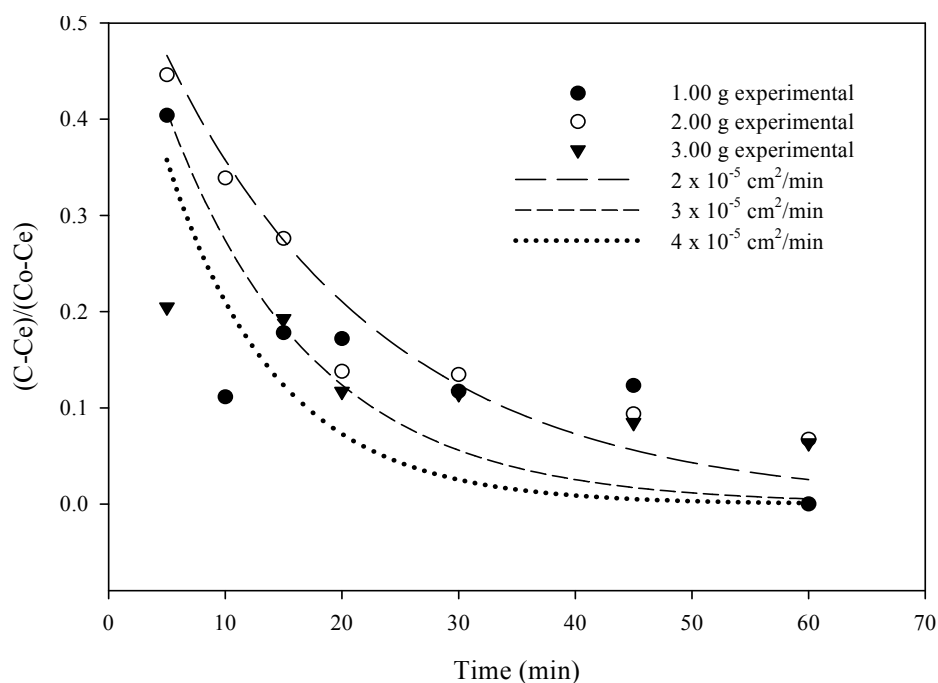


Figure 4-12 Experimental and fitted results of perchlorate adsorption on loose resin during the first 60 minutes. The fitted lines plot the analytical solutions obtained by trial and error of the diffusion coefficient.

Using this method the diffusion coefficient was estimated between 2×10^{-5} and $4 \times 10^{-5} \text{ cm}^2/\text{min}$. A study from Xiong et al. (2007) on the sorption of perchlorate on several IX resins established that the intraparticle diffusion coefficient varied between 2.5×10^{-7} and $7.5 \times 10^{-6} \text{ cm}^2/\text{min}$. The authors concluded that the diffusion coefficient for the resin with the highest selectivity and capacity (A530E) was $1.25 \times 10^{-6} \text{ cm}^2/\text{min}$. On the other hand, the reported diffusion coefficient of perchlorate at infinite dilution is $1.074 \times 10^{-3} \text{ cm}^2/\text{min}$ ($1.79 \times 10^{-5} \text{ cm}^2/\text{s}$) (Hristovski et al., 2008; Lide, 2006).

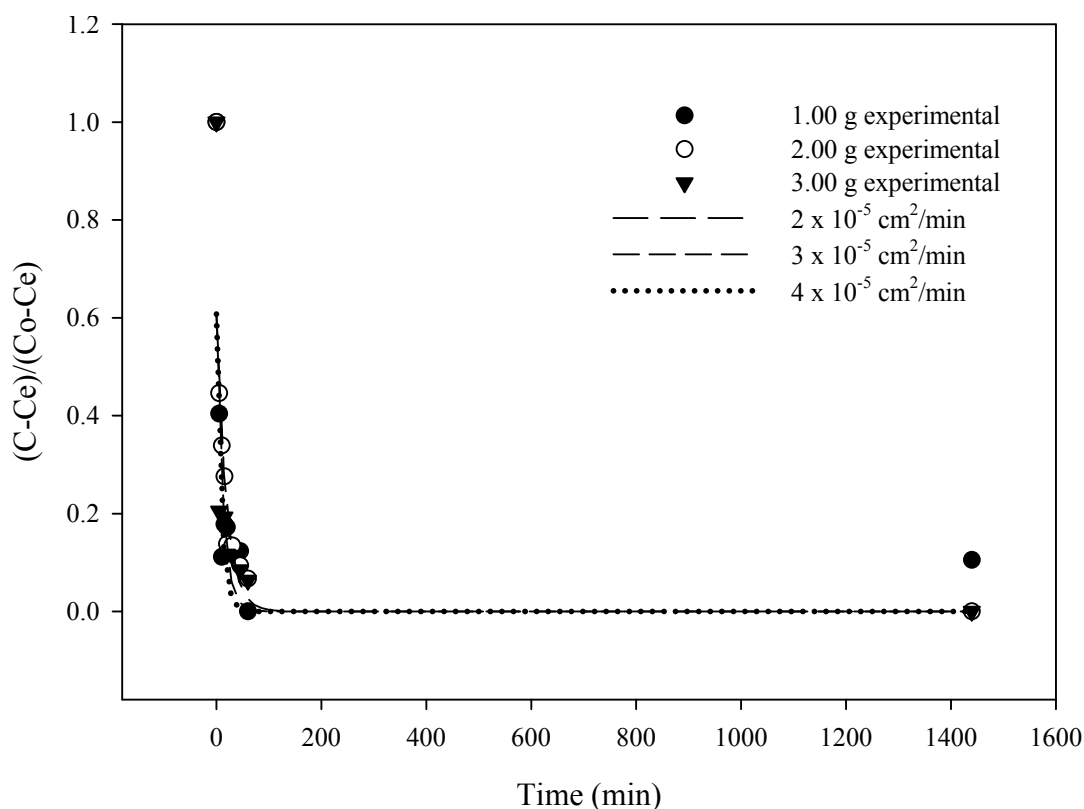


Figure 4-13 Experimental and fitted results of perchlorate adsorption on loose resin during the first 1440 minutes (24hr). The fitted lines plot the analytical solutions obtained by trial and error of the diffusion coefficient.

The diffusion of perchlorate within the pores of the studied resin is of the same order of magnitude as the reported diffusion coefficient of perchlorate in solution at infinite dilution and up to ten orders of magnitude higher than the reported diffusion coefficients of the resins studied by Xiong et al. (2007).

A similar method was used to determine the diffusion coefficients of perchlorate desorption from the exhausted resin. Desorption experiments were carried out by placing

the exhausted resin into a 6% NaCl solution. Figure 4-14 below shows the results for the diffusion coefficients during the first 60 minutes.

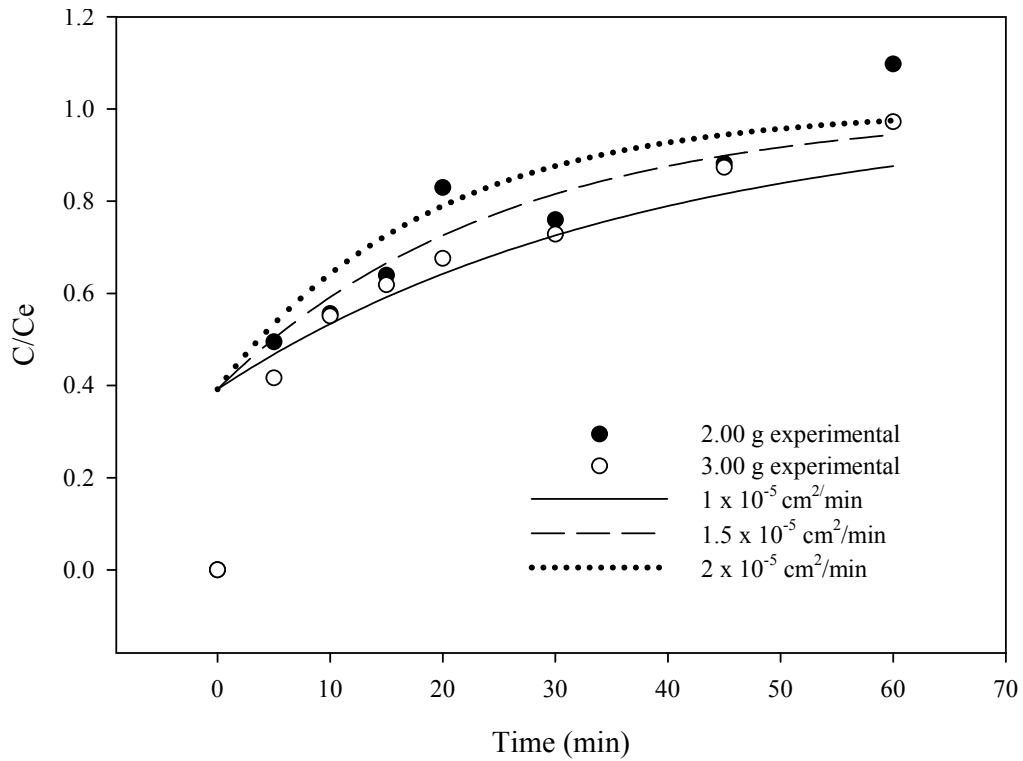


Figure 4-14 Experimental and fitted results of perchlorate desorption on loose resin during the first 60 minutes. The fitted lines plot the analytical solutions obtained by trial and error of the diffusion coefficient.

Form Figure 4-14 the estimated intraparticle diffusion coefficients of perchlorate desorption is between 1.5×10^{-5} and 2.5×10^{-5} cm^2/min . These results are of the same order of magnitude as the adsorption coefficients obtained for the adsorption experiments.

4.4.2 Adsorption Kinetic Models

The sorption process can be based on the chemical reaction adsorption process, the mass transfer process or a combination of both. A number of adsorption kinetic models were tested in order to better understand the controlling mechanisms; the models were presented in section 2.4.2 and include four adsorption reaction models and four adsorption diffusion models. The following is a discussion of each model tested and at the end of the section Table 4-4 summarizes the results. Experimental data collected from the adsorption of perchlorate onto 1.00 g, 2.00 g and 3.00 g of loose resin during the first 60 minutes was used to test the models.

4.4.2.1 Pseudo-First Order Kinetic Model

The pseudo-first order model is applicable to the early stages of the process, up to 20% uptake. After a high surface loading there is a considerable change in the adsorbate concentration in the solution and a reduction of the resin's available sites for adsorption making the model less applicable (Shek et al., 2009). Figure 4-15 presents the results of applying the model to the experimental data. Low correlation coefficients were obtained varying from 0.45, 0.69 and 0.84 for the 1.00 g, 2.00 g and 3.00 g of resin respectively. Also, there is a large difference between the experimental and calculated values of the experimental equilibrium concentration q_e and the equilibrium concentration parameter q_{ecal} for each set of data, which show a poor pseudo-first order fit of the experimental data. The results are presented in Table 4-4.

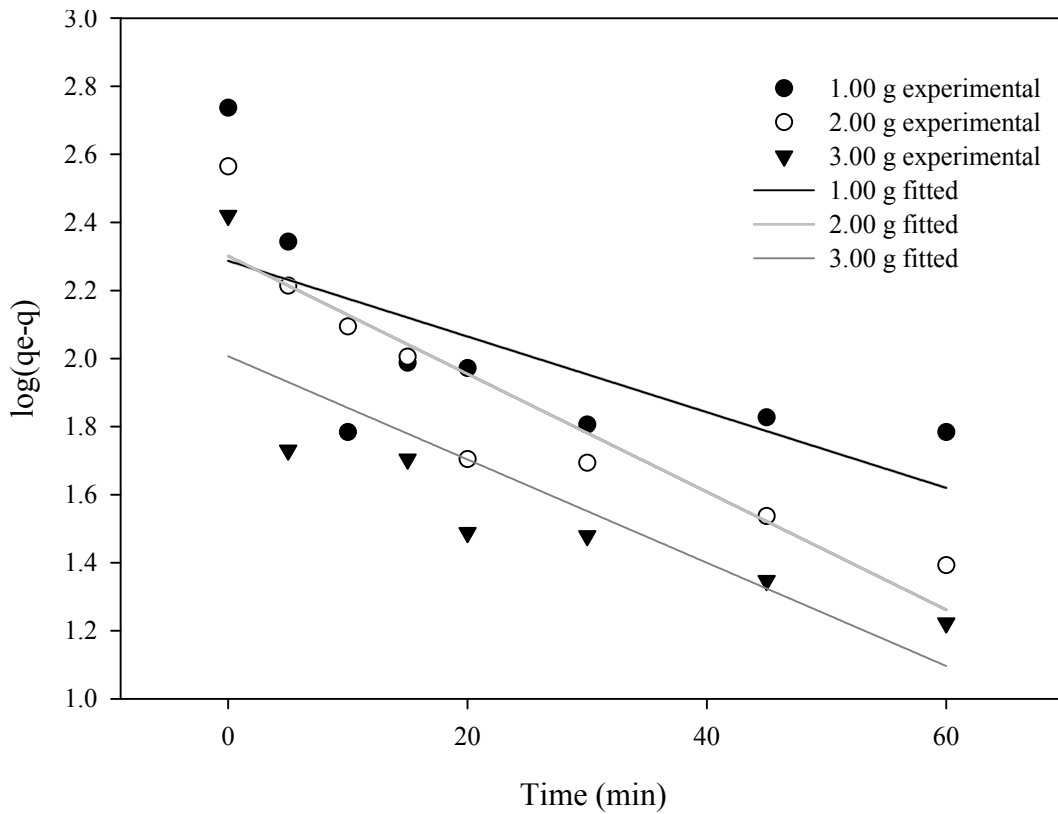
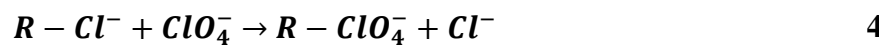


Figure 4-15 Pseudo-first order kinetics of perchlorate adsorption onto loose resin.

4.4.2.2 Pseudo-Second Order Kinetic Model

Ho and McKay (1999) developed an equation based on the assumption that chemisorptions occur through the exchange of electrons between the adsorbent and adsorbate and that it may be described by a second order equation. The ion exchange reaction taking place on the surface of the resin can be expressed as:



-4

The rate of adsorption described by equation 4-4 depends on the amount of perchlorate ions on the resin surface at time t and the amount of ions adsorbed at equilibrium (Qui et al., 2009; Ho, 2006).

Since the calculated correlation coefficients of the three sets of data presented on Figure 4-16 are consistent and higher than 0.998, the adsorption kinetics of perchlorate on the resin can be explained by the pseudo-second order kinetics model and not by intraparticle diffusion, which indicates that chemisorption is the controlling mechanism. The chemical process of the exchange of ClO_4^- ions for Cl^- ions is the rate limiting step. A research conducted by Tripp (2001) comparing 17 commercially available resins concluded that the ones with macroporous matrix with the most hydrophobic functional group had higher affinities for perchlorate since it is a large ion ($58.8 \text{ cm}^3/\text{g-mole}$) classified as poorly hydrated (Batista et al., 2002). The parameters of the pseudo-second order model were calculated and are presented in Table 4-4.

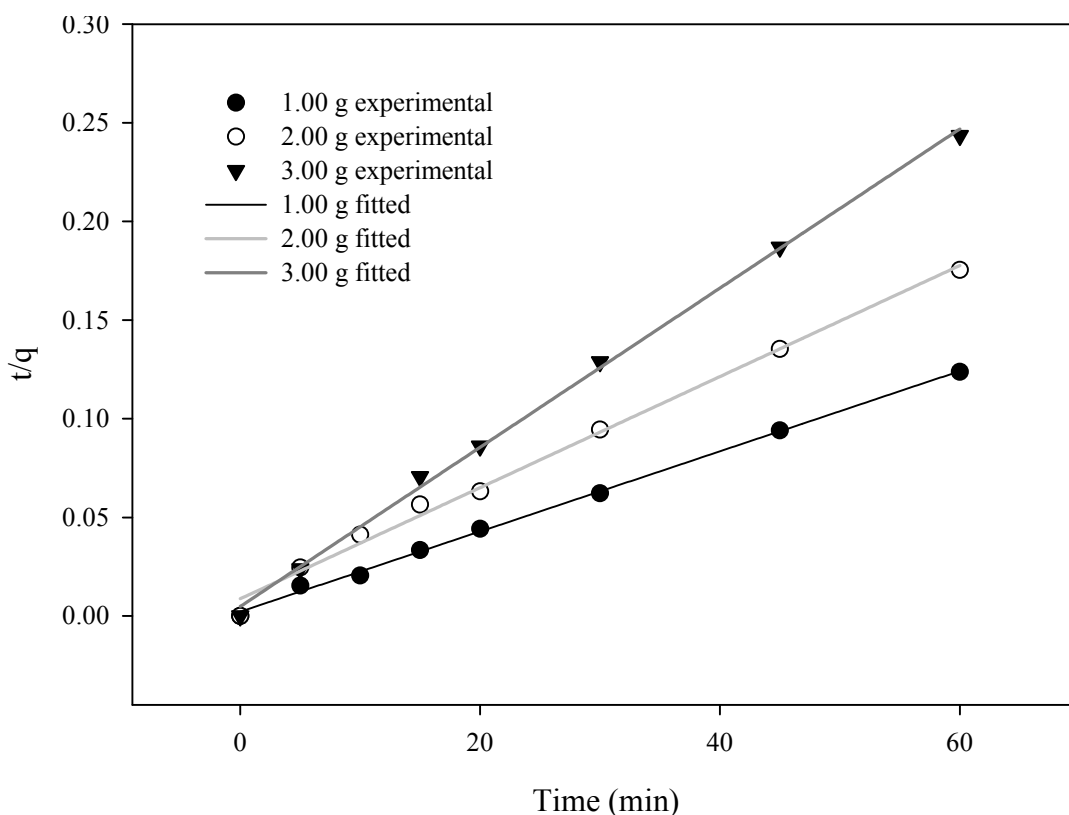


Figure 4-16 Pseudo-second order kinetics of adsorption of perchlorate onto loose resin.

4.4.2.3 Elovich's Equation

Elovich's equation is also a type of chemisorption model but does not predict any definite mechanism (Kumar et al., 2011). The model is useful in describing adsorption on highly heterogeneous adsorbents. The correlation coefficient for 1.00 g data is very low (0.56), higher values of the coefficient were obtained for 2.00 g and 3.00 g (0.94 and 0.87 respectively). There is high variation between the values of the estimated parameters for each data set showing little consistency for the model as shown in Figure 4-17.

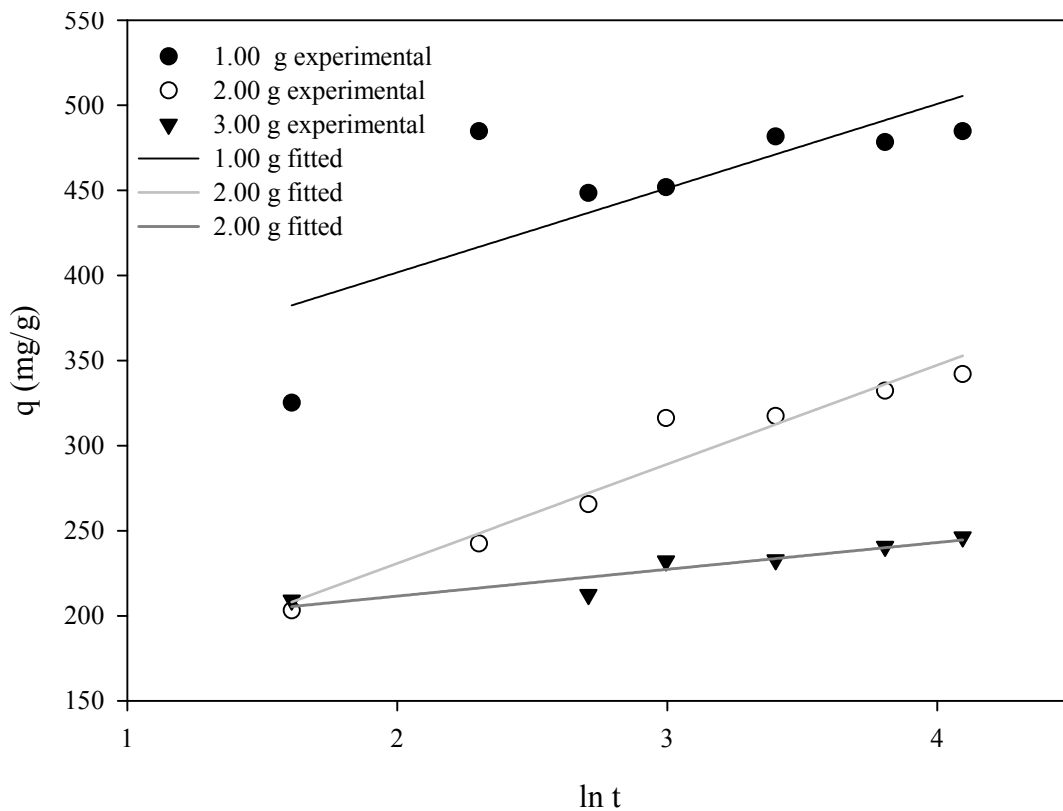


Figure 4-17 Elovich's model of adsorption of perchlorate onto loose resin.

4.4.2.4 Second-Order Rate Equation

Figure 4-18 presents the experimental and fitted results of applying the second order rate equation. The correlation coefficients obtained were low, 0.41, 0.78 and 0.65 for 1.00 g, 2.00 g and 3.00 g, respectively. The estimated parameters are presented in Table 4-4.

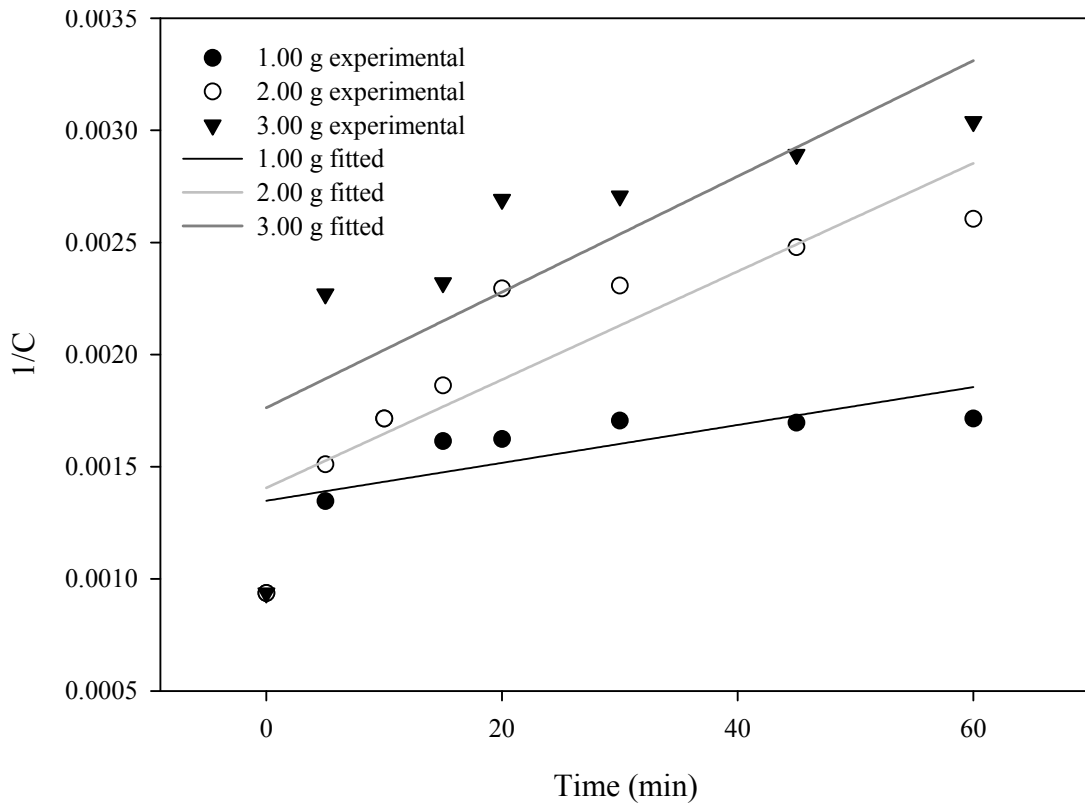


Figure 4-18 Second order kinetics of adsorption of perchlorate onto loose resin.

The rate constants and correlation coefficients of the four adsorption reaction models tested are presented in Table 4-4.

The results clearly show that the experimental data is best described by the pseudo-second order model. The correlation coefficients for all the resin masses tested are above 0.998. The correlation coefficients of the other three models are lower than those of the pseudo-second order model, suggesting that the rate limiting stage for the adsorption of perchlorate into the IX resin may be chemisorption.

Table 4-4 Parameters of adsorption reaction kinetic models applied to the adsorption of perchlorate onto loose resin experiments.

Kinetic model	Parameters		Resin mass		
			1.00 g	2.00 g	3.00 g
Pseudo-first order	kp1	(min ⁻¹)	5.3	5.3	4.6
	qecal	(mg/g)	0.975	0.961	0.966
	R ²		0.454	0.849	0.694
	kp2	(g/mg/min)	1.8E-03	8.9E-04	3.3E-03
Pseudo second order	qecal	(mg/g)	492.1	357.1	250.0
	R ²		0.999	0.998	0.999
	ln(aα)	(min ⁻¹)	9.1	0.1	5913
Elovich's equation	α	(mg/g/min)	49.5	58.3	15.7
	R ²		0.558	0.938	0.868
	k2	(L/mg/min)	8.4E-06	2.4E-05	2.6E-05
Second order equation	Ce	(mg/L)	742	711	567
	R ²		0.406	0.779	0.623

A normalization of the pseudo-second order rate constant k_{p2} by the weight of resin on each experiments results in the following values for 1.00 g, 2.00 g and 3.00 g respectively; 1.8×10^{-3} , 1.6×10^{-3} and 1.1×10^{-3} (1/mg/min) with an average of 1.5×10^{-3} (1/mg/min) and a standard deviation of 3.9×10^{-4} .

Although the results could be described very well by the chemisorption type of model, intraparticle diffusion models were also tested to verify the influence of mass transfer resistance.

4.4.2.5 Film Diffusion Mass Transfer Rate

The correlation coefficients of modeling the experimental data with the film diffusion mass transfer were 0.454, 0.694 and 0.849 for 1.00 g, 2.00 g and 3.00 g of resin respectively. As presented in the literature review this model is similar to the pseudo-first

order kinetic model, however in agitated adsorption studies, film diffusion is usually controlling only for the first few minutes (Ho et al., 2010). Figure 4-19 presents the experimental and fitted results.

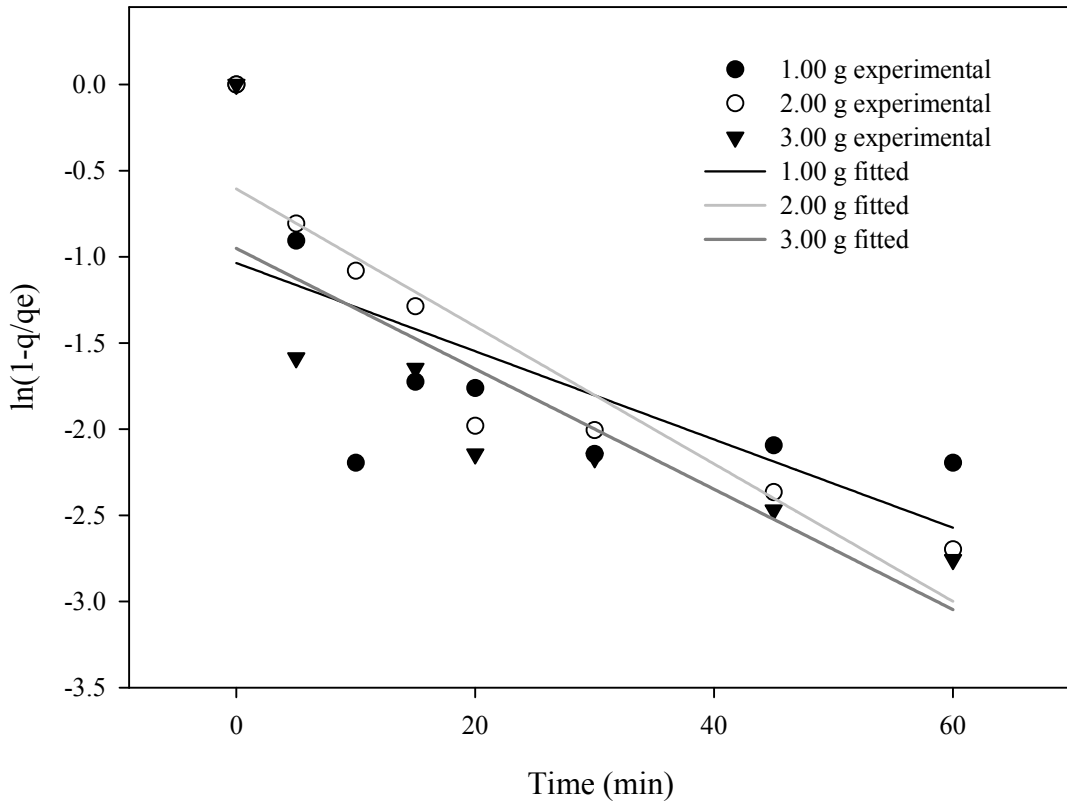


Figure 4-19 Film diffusion mass transfer rate model of adsorption of perchlorate onto loose resin.

4.4.2.6 Weber-Morris Model

The adsorption process would be controlled solely by intraparticle diffusion if the plot of q_t versus $t^{1/2}$ is linear and passes through the origin. Figure 4-20 shows that none of these conditions applied to any of the tests. The correlation coefficients were 0.429,

0.858 and 0.889 for 1.00 g, 2.00 g and 3.00 g respectively. All the fitted lines show an intercept of the plot which reflects the boundary layer effect (Kumar et al., 2011). This effect appears larger for the test with the smallest amount of resin and is almost half for the other two amounts.

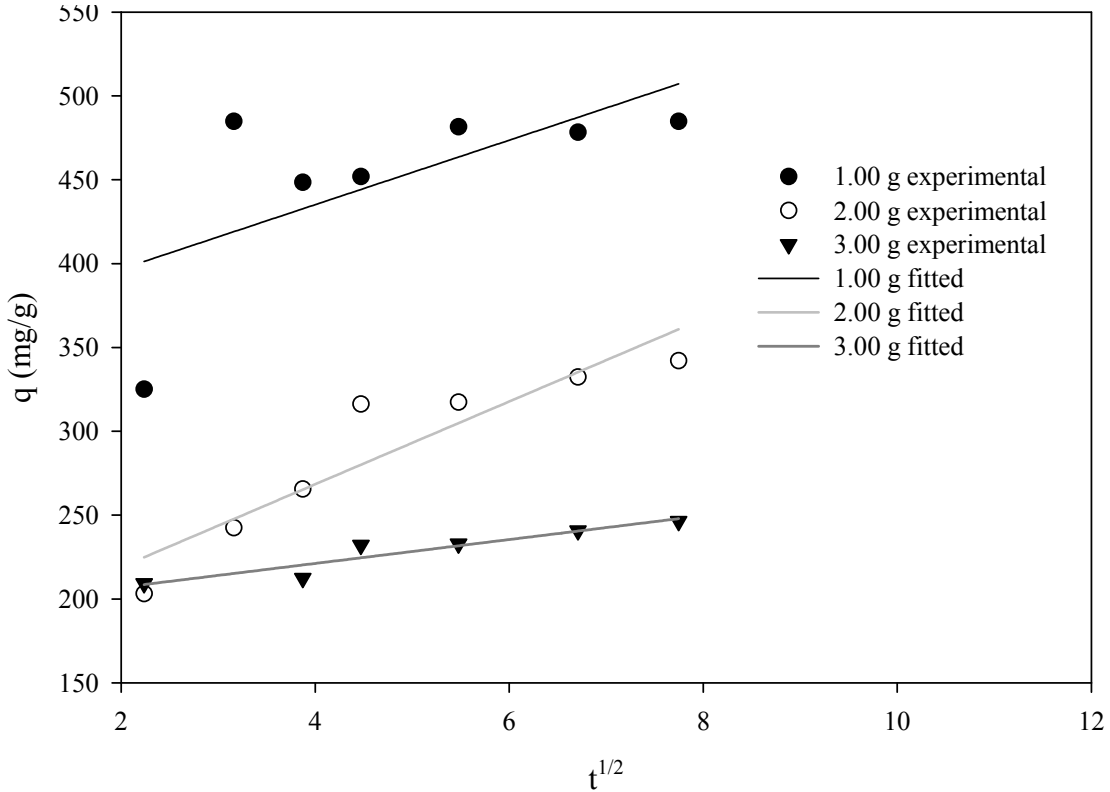


Figure 4-20 Weber-Morris model of adsorption of perchlorate onto loose resin.

4.4.2.7 Dumwald-Wagner Model

A linear plot of this model provides a rate constant K (min^{-1}) obtained from the slope shown in Figure 4-21. The correlation coefficients did not show a good fit as shown in Table 4-5. The 2.00 g test had the best fit with a correlation coefficient of 0.908 and the 1.00 g test had the lowest coefficient (0.485). The rate constant coefficient estimated

ranged from 8.5×10^{-3} to $1.4 \times 10^{-2} \text{ min}^{-1}$. This model provides further confirmation that the adsorption process is not solely controlled by intraparticle diffusion.

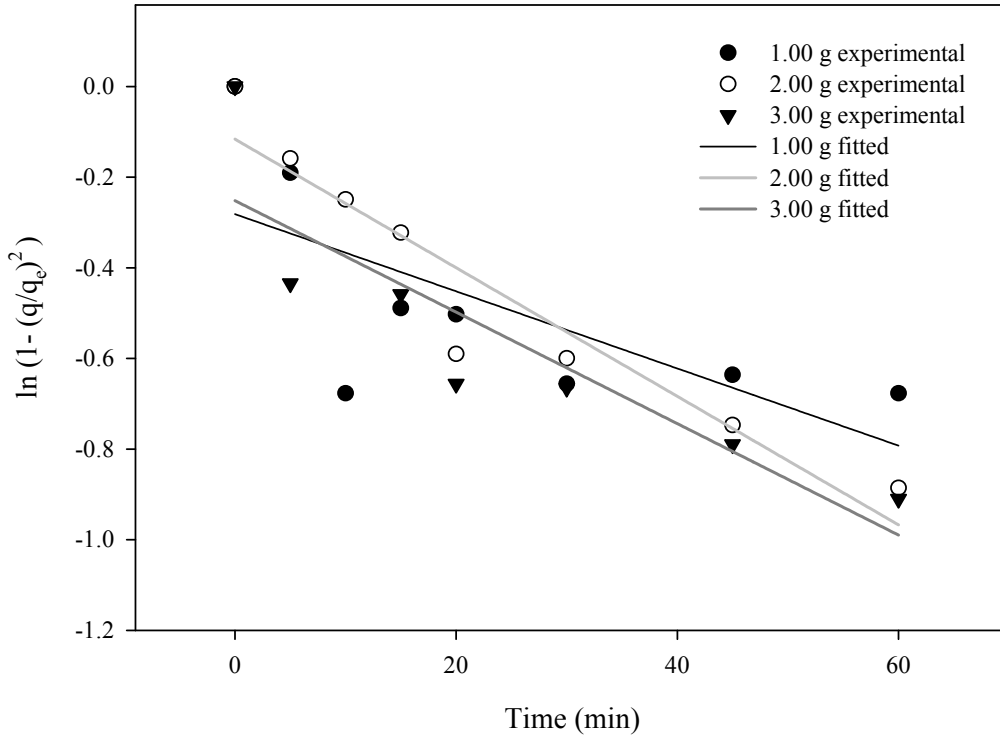


Figure 4-21 Dumwald-Wagner model of adsorption of perchlorate onto loose resin.

4.4.2.8 Boyd Kinetic Model

The Boyd kinetic model allows identifying the slowest stage between film diffusion and intraparticle diffusion. A plot of Bt versus t that is linear but does not pass through the origin is an indication of a process controlled by film diffusion. Figure 4-22 presents the results of applying this plot to the experimental data. The calculated B values can then be used to estimate the effective diffusion coefficient, D_i (cm^2/min) with equation 2-31.

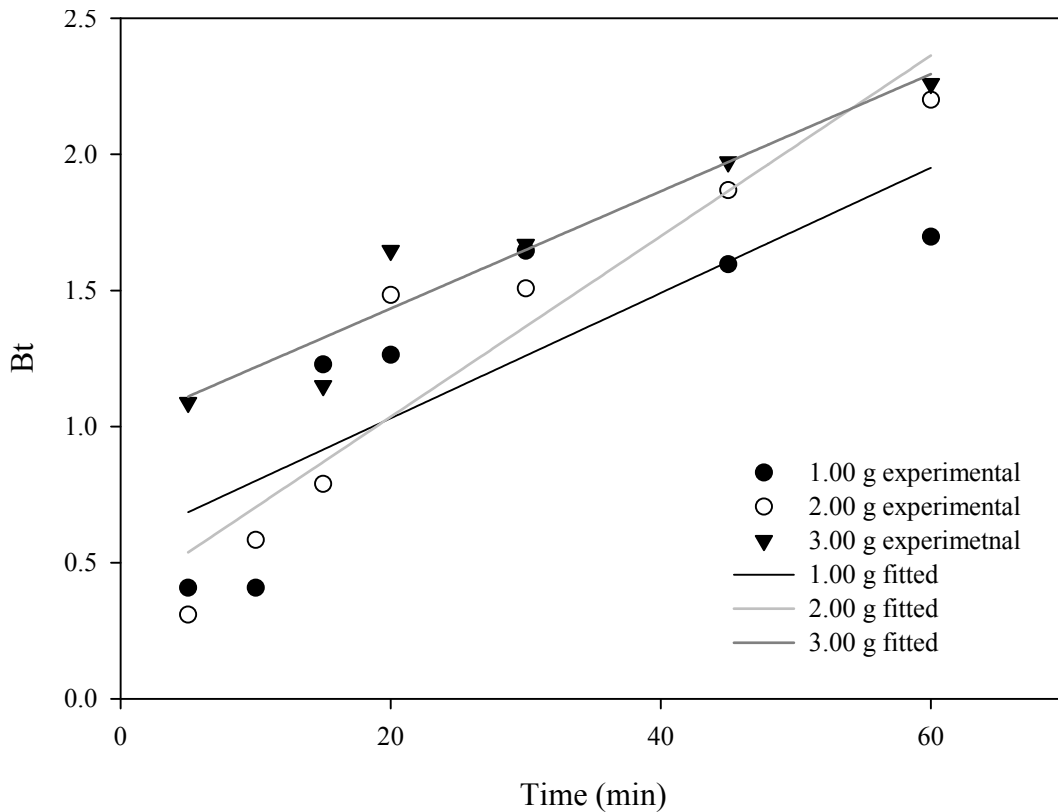


Figure 4-22 Boyd kinetic model of adsorption of perchlorate onto loose resin.

Table 4-5 presents the results of the estimated effective diffusion coefficients calculated for the first 60 minutes of data. It is noticeable that the calculated values are in good agreement with those estimated in section 4.4.1 by trial and error when only considering an intraparticle diffusion controlled process. The estimated values in section 4.4.1 were 2.5×10^{-5} , 3.5×10^{-5} , and 4.5×10^{-5} cm^2/min compared the Boyd kinetic model of 2.1×10^{-5} , 2.0×10^{-5} , and 3.2×10^{-5} cm^2/min for 1.00 g, 2.00 g and 3.00 g of loose resin respectively.

Table 4-5 Parameters of adsorption diffusion models applied to the adsorption of perchlorate onto loose resin experiments.

Kinetic model	Parameters	Resin mass			
		1.00 g	2.00 g	3.00 g	
Film diffusion mass transfer rate	R ¹	-2.6E-02	-4.0E-02	-3.5E-02	
	R ²	0.454	0.849	0.694	
	C	358	170	193	
Weber-Morris model	k _{int}	mg/g/min ^½	19.2	24.7	7.13
	R ²		0.429	0.858	0.889
			-2.8E-01	-1.2E-01	-2.5E-01
Dumwald-Wagner model	K	min ⁻¹	-8.5E-03	-1.4E-02	-1.2E-02
	R ²		0.485	0.908	0.790
			2.1E-05	2.0E-05	3.2E-05
Boyd kinetic model	D _i	cm ² /min			
	R ²		0.680	0.892	0.924

None of the adsorption diffusion models tested showed a good fit of the experimental data, which contradicts the initial hypothesis that the adsorption of perchlorate in an agitated batch process was controlled exclusively by intraparticle diffusion. The results show an effect of the liquid film on the process and it was characterized by estimating an effective diffusion coefficient D_i .

From all the models tested only the pseudo-second order kinetic model was able to reproduce the experimental results. This model characterizes a process controlled by the ion exchange reaction taking place between the perchlorate ions in solution and the chloride ions in the resin.

4.4.3 Desorption Kinetic Models

Based on these findings the pseudo-second order and Boyd kinetic models were applied to the experimental data for perchlorate desorption in which the resin was contained inside the membrane. Understanding the mass transfer mechanism for the perchlorate desorption is important since the biological regeneration was carried out with this set up.

Figure 4-23 shows the experimental and fitted results for applying the pseudo-second order rate equation. Equation 2-16 was rewritten to represent desorption of perchlorate from the resin with an initial concentration q_0 (mg/g):

$$\frac{dq_t}{dt} = k_{d2}(q_t - q_e)^2. \quad 4-5$$

Rearranging and integrating equation 4-9 with boundary conditions $q_t=q_0$ at $t=0$ and $q_t=q_t$ at $t=t$ yields:

$$\frac{1}{q_t} \left[\frac{1}{bk_{d2}} + t \right] = \frac{1}{q_e} t + \frac{1}{bk_{d2}q_e}, \quad 4-6$$

where:

k_{d2} is the pseudo-second order rate constant for the desorption kinetic model (g/mg/min),

b is $(q_0 - q_e)$, the difference between the initial and equilibrium concentration of perchlorate in the resin.

Equation 4-10 was simplified assuming that:

$$\frac{1}{bk_{d2}} \cong 0, \quad 4-7$$

Then equation 4-10 can be written as:

$$\frac{t}{q_t} = \frac{1}{q_e} t + \frac{1}{bk_{d2}q_e} \quad 4-8$$

A plot of t/q_t against t can be used to determine the pseudo-second order rate constant of desorption k_{d2} (mg/g/min). Then the assumption shown in equation 4-7 was tested and confirmation was obtained that ignoring this term of the equation was reasonable.

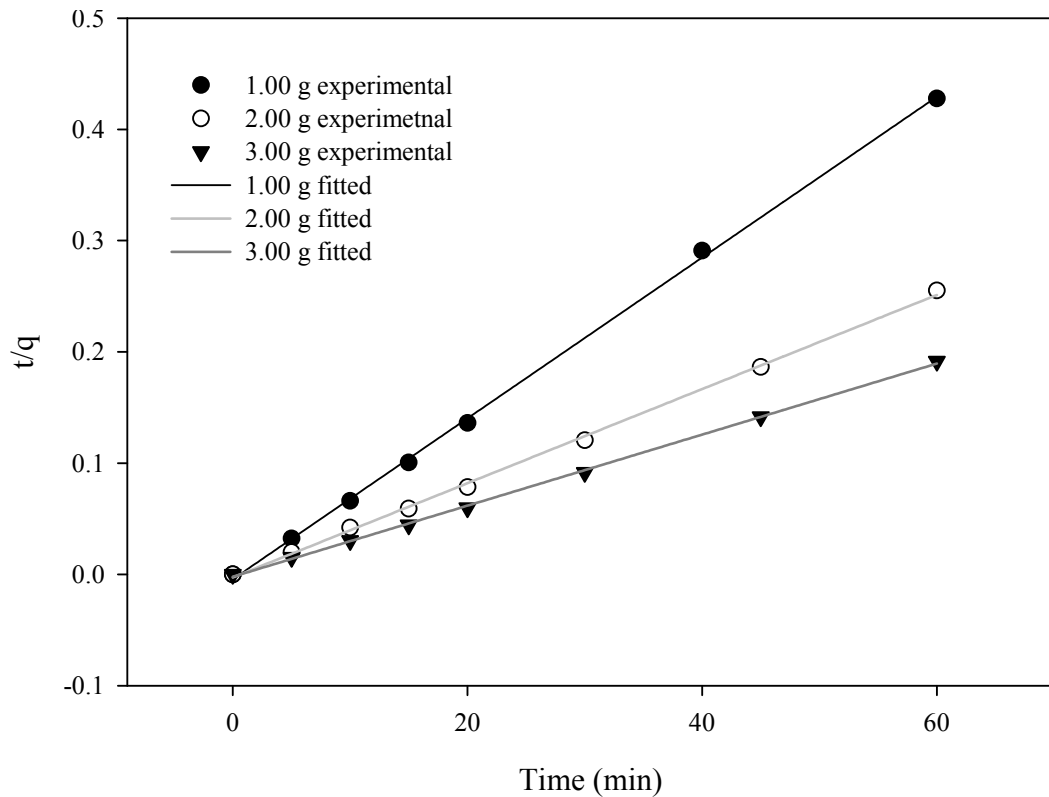


Figure 4-23 Pseudo-second order rate model of desorption of perchlorate from resin inside the membrane and 6% NaCl solution.

The correlation coefficients of the fitted lines are all higher than 0.99 as presented in Table 4-6. The pseudo-second order model rate constant k_{d2} is negative because perchlorate is desorbing from the resin. The values of the desorption rate constants are: -7.8×10^{-2} , -4.1×10^{-2} and -3.9×10^{-2} , for 1.00 g, 2.00 g and 3.00 g respectively. If normalized by the resin mass the desorption rate constant are: -7.8×10^{-2} , -2.0×10^{-2} and -1.3×10^{-2} , for 1.00 g, 2.00 g and 3.00 g respectively, averaging -3.7×10^{-2} (1/mg/min). The results show that desorption of perchlorate from the resin contained inside the membrane can be modeled as a process controlled by chemisorption.

The Boyd kinetic model was also tested to verify the liquid film and intraparticle diffusion mechanisms. Equation 2-28 was modified as presented below to represent the desorption process:

$$Bt = -0.4977 - \ln(F). \quad \mathbf{4-9}$$

Figure 4-24 shows a plot of the experimental data and fitted results. The results show a poor correlation for the experiments with 2.00 g and 3.00 g of resin; the correlation for the 1.00 g was 0.979. If the fitted plots are linear and pass through the origin, then the slowest stage is intraparticle diffusion, since this is not the case the process is not controlled purely by intraparticle diffusion as was initially stated in the hypothesis.

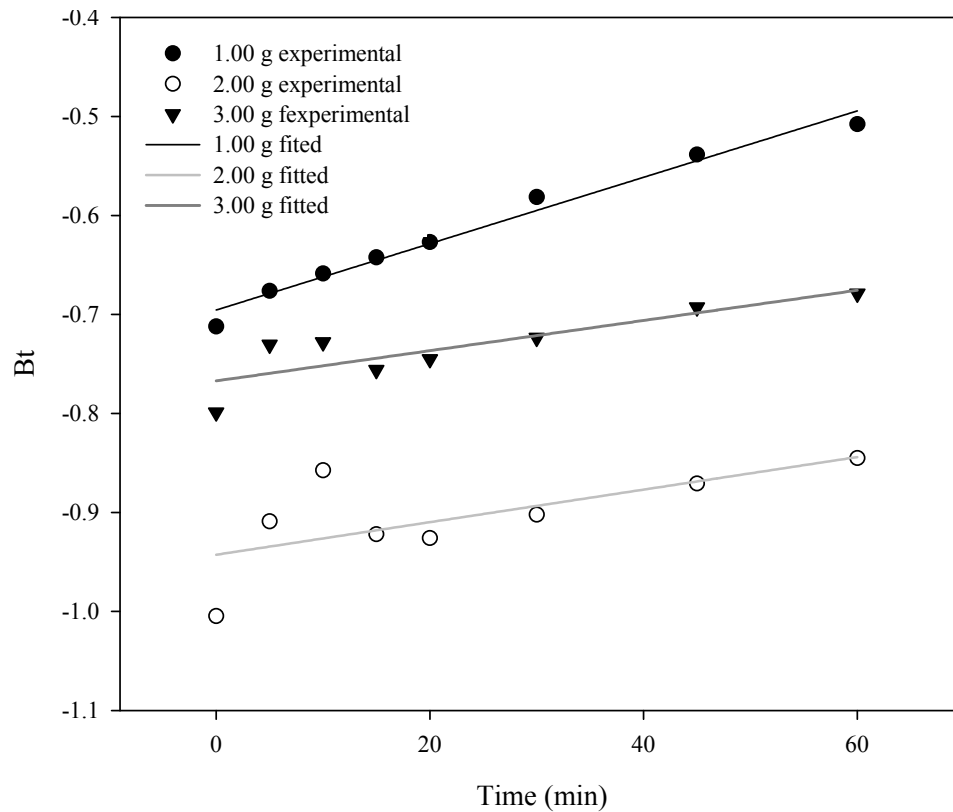


Figure 4-24 Boyd kinetic model of perchlorate desorption from resin inside the membrane and 6% NaCl solution.

Table 4-6 presents the estimated parameters for the two models tested. The estimated effective diffusion coefficients determined from the Boyd kinetic model are 1.7×10^{-5} , 2.4×10^{-5} and 1.9×10^{-5} (cm^2/min) for 1.00 g, 2.00 g and 3.00 g respectively with an average of 2.0×10^{-5} and a standard deviation of 3.4×10^{-6} . These results compared with the diffusion coefficient obtained on section 4.4.1 by trial and error between 1.5×10^{-5} and 2.5×10^{-5} cm^2/min .

Table 4-6 Parameters of kinetic models applied to the desorption of perchlorate from the resin inside the membrane.

Kinetic model	Parameters	Resin mass			
		1.00 g	2.00 g	3.00 g	
Pseudo second order	kd2	(g/mg/min)	-7.8E-02	-4.1E-02	-3.9E-02
	qecal	(mg/g)	138.4	236.4	313.2
	R ²		0.999	0.999	0.999
Boyd kinetic model	Di	cm ² /min	1.8E-05	2.4E-05	1.9E-05
	R ²		0.979	0.459	0.723

The results from the equilibrium studies and the kinetic model findings were applied to the experiments on the biological regeneration of exhausted resin enclosed in a membrane and placed in the NP30 culture.

4.5 Biological Regeneration of Exhausted Resin

For this study eight biological degradation experiments were prepared. The set up in Figure 4-25 consisted of perchlorate exhausted resin inside a membrane and placed in an Erlenmeyer containing 200 mL of NP30 culture in a prepared medium with the composition shown in the materials and methods section.



Figure 4-25 Biological degradation experimental set up.

Samples from each one of the eight experiments were taken at established time intervals to measure the perchlorate concentration as described in section 3.6.4 of the materials and methods. Figure 4-26 presents the results from the biological regeneration experiment. The perchlorate concentration in the solution increased within the first hour and then decreased rapidly within the next 24 hours. After this initial period, the concentration of perchlorate remained stable.

A model was developed using Excel© to simulate the results. For this model the desorption of perchlorate from the resin inside the membrane was estimated using the pseudo-second order equation presented and discussed in section 4.4.3, with a desorption rate constant of -7.8×10^{-2} mg/g/min. Since the mass of resin and volume of solution were determined from the beginning of the experiment, the slope of the operating line was known. Also known was the equilibrium line function in the form of Freundlich model from the isotherm experiments in section 4.2.

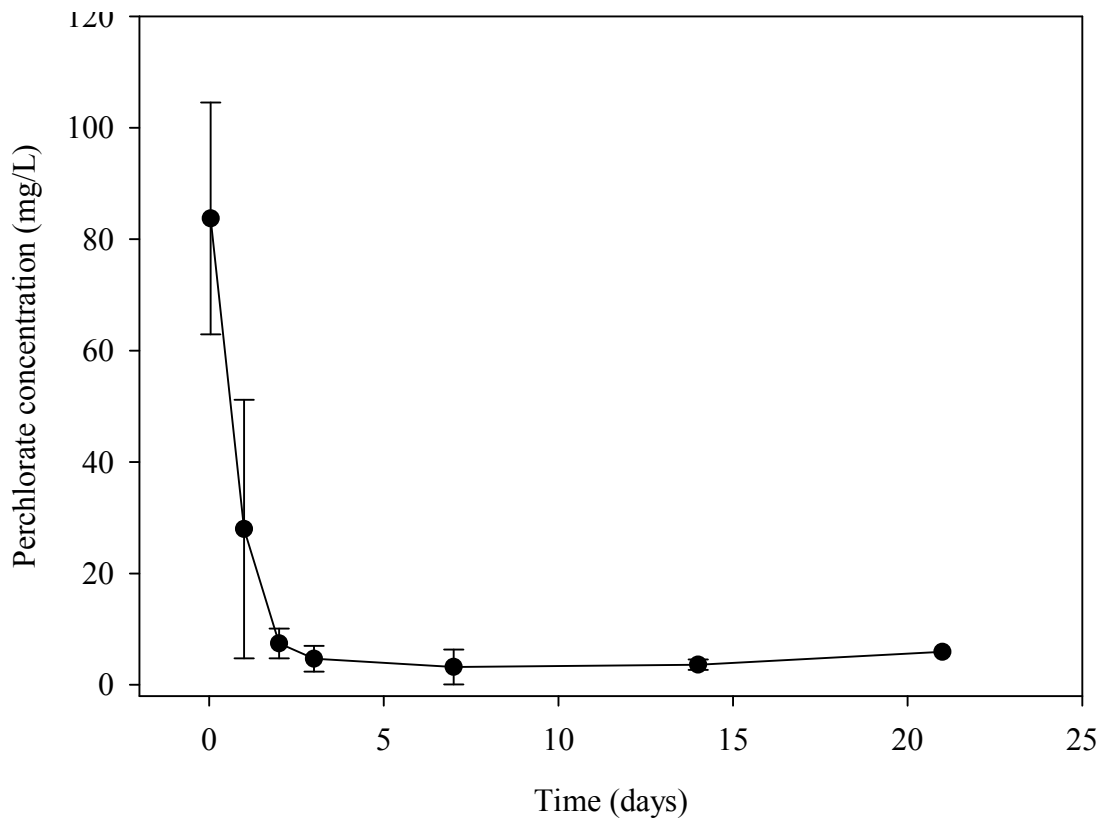


Figure 4-26 Biological regeneration of exhausted SBA resin using NP30 culture at 20°C. One replicate was killed after sampling. Initially seven replicates.

With these two equations (equilibrium and operating line) the coordinates of the point where the two lines cross (q_{e1}, C_{e1}), was determined given the value the concentration of perchlorate in liquid and solid phase at equilibrium for an initial solid phase concentration q_0 and the initial solution concentration $C_0 = 0$.

With the calculated coordinates (q_{e1}, C_{e1}), and the amount of perchlorate desorbed as a function of time, biomass concentration, rate of biodegradation, amount of perchlorate biodegraded (C_{b1}) and amount of perchlorate left in solution were estimated using the following equations:

$$\frac{dX}{dt} = Y \frac{dS}{dt}, \quad 4-10$$

$$v = V \frac{v_m SX}{K_s + S}, \quad 4-11$$

where:

Y is the biomass yield (mg VSS/ mg ClO₄⁻),

X is the biomass concentration (mg VSS/L),

v is the specific perchlorate reduction rate (ClO₄⁻/mg VSS·h),

v_m is the maximum specific perchlorate reduction rate (mg ClO₄⁻/mg VSS·h),

K_s is the half saturation constant (mg ClO₄⁻/L),

S is the substrate concentration (mg/L).

This type of model was previously applied by Xiao et al. (2010) for culture NP30. The author estimated a half saturation coefficient of 26 ± 2 mg/L and maximum reduction rate of (4.3 ± 0.41) × 10⁻³ mg ClO₄⁻/mg VSS·h and a yield of 0.06 mg VSS/ mg ClO₄⁻ for the model presented in equations 4-10 and 4-11. A time step of 5 minutes was used to perform the calculations.

As the culture degrades perchlorate desorbed from the resin the operating line shifts to the left thus requiring a recalculation of the coordinates where the new line crosses the

equilibrium (q_{e2}, C_{e2}) . The concentration of perchlorate in the resin would be the same as for the previous operating line (q_1) , but the concentration of perchlorate in the solution is less because of the amount degraded $(C_1 - C_{b1})$. This procedure is repeated for a delta of time until the equilibrium is reached (q_{en}, C_{en}) . The described procedure is represented in the Figure 4-27, the arrows follow the sequence in which the model was calculated.

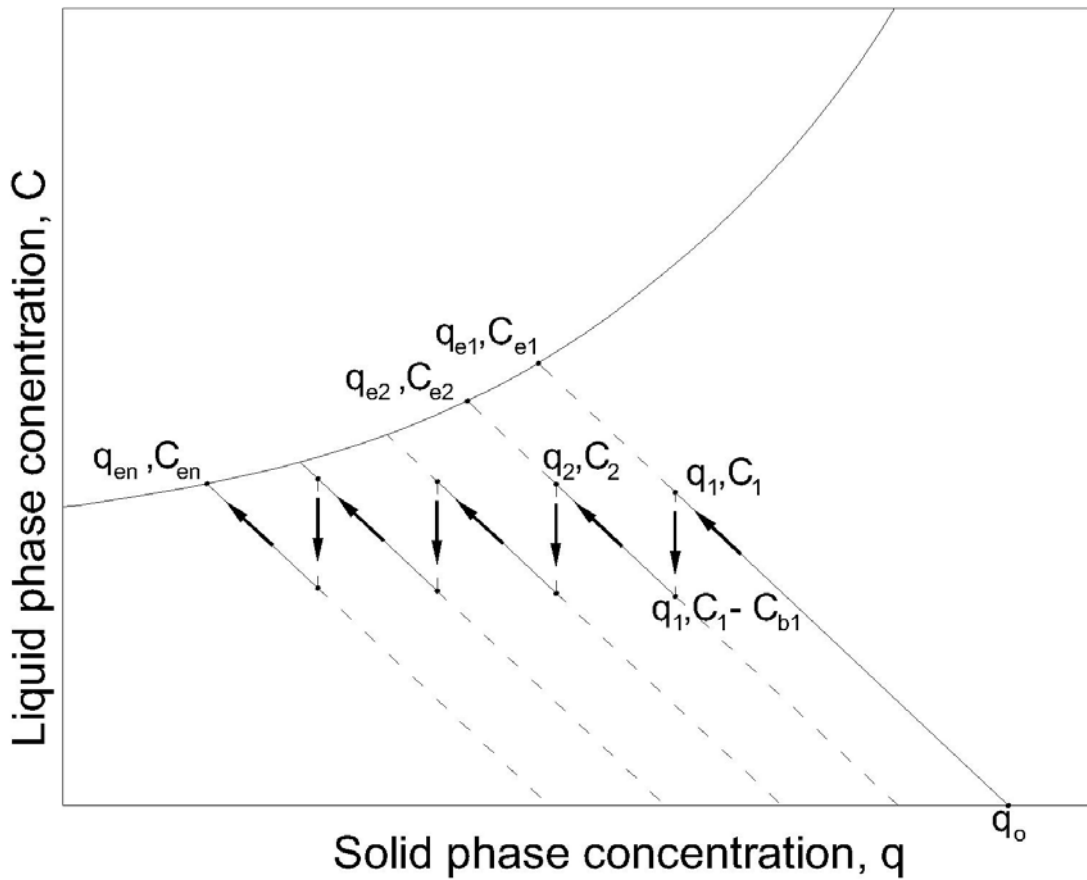


Figure 4-27 Operating diagram of the biological degradation process of perchlorate desorbed from the resin.

Appendix A presents a sample of the first 120 minutes of the Excel© spreadsheet calculation performed to model the desorption and biological regeneration of perchlorate from exhausted SBA resin when placed inside the membrane. Columns labeled q_e and C_e are the ones calculating the new equilibrium concentration by trial and error for each delta of time. When running the model it was found that the model is sensitive to the Freundlich adsorption intensity parameter n . A change on this parameter affects the convexity of the equilibrium function. As a result the Freundlich adsorption intensity parameter was modified from 2.36 to 4.0 to better simulate the results.

Figure 4-28 shows the entirety of the results for the 21 days of duration of the experiment. The results are comparable to those of the experimental data. The highest concentration of perchlorate detected in any of the samples taken during the experiment corresponds to the one taken at 1 hour. The model shows this increase in the amount of perchlorate in the solution for the first 40 minutes as seen in the data presented on Appendix A, followed by a rapid decline of perchlorate concentration despite the fact that perchlorate is still being desorbed.

The rate of perchlorate degradation by NP30 culture is responsible for this decline. This proves that the culture is capable of regenerating the exhausted resin even though is not in direct contact with it. The perchlorate desorbed crosses the membrane and is available as an electron acceptor for the NP30 culture allowing it to thrive as shown in the modeled results presented.

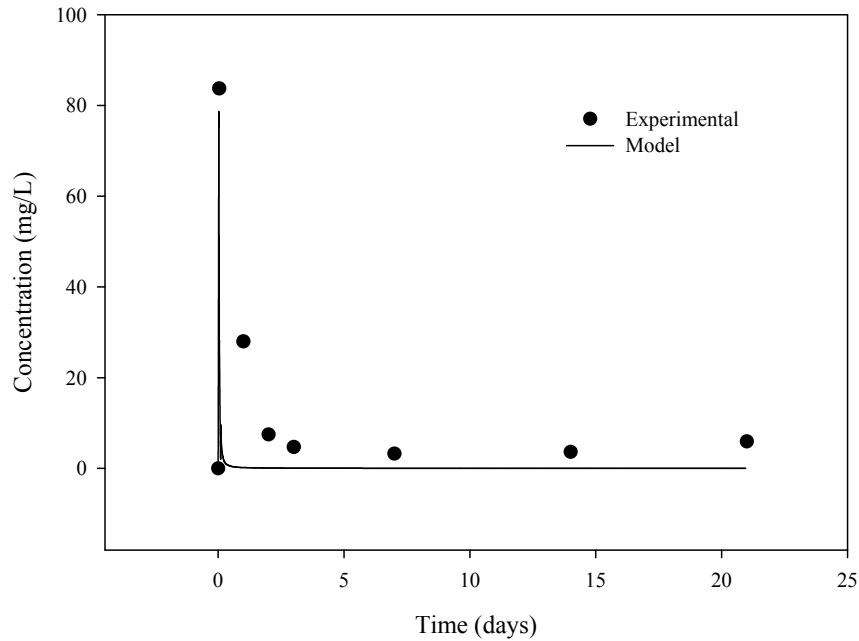


Figure 4-28 Model and experimental results for the desorption and biological regeneration of perchlorate exhausted resin contained inside a membrane.

The operating diagram shown in Figure 4-29 presents the equilibrium function and a plot of the results of the estimated concentration of perchlorate in solution (column q_n versus C_{left} in Appendix A). The dotted lines represents the theoretical operating line of the desorption of perchlorate from the resin inside the membrane but with no biological regeneration. Once it reaches equilibrium there is no net change in perchlorate concentration in the solution. On the other hand, the dashed curve represents the process in which the culture is degrading perchlorate as it desorbs from the resin. By doing this, the culture “shifts” the equilibrium allowing for more perchlorate to leave the resin. The desorbed perchlorate is rapidly degraded because the dashed line follows the equilibrium line closely.

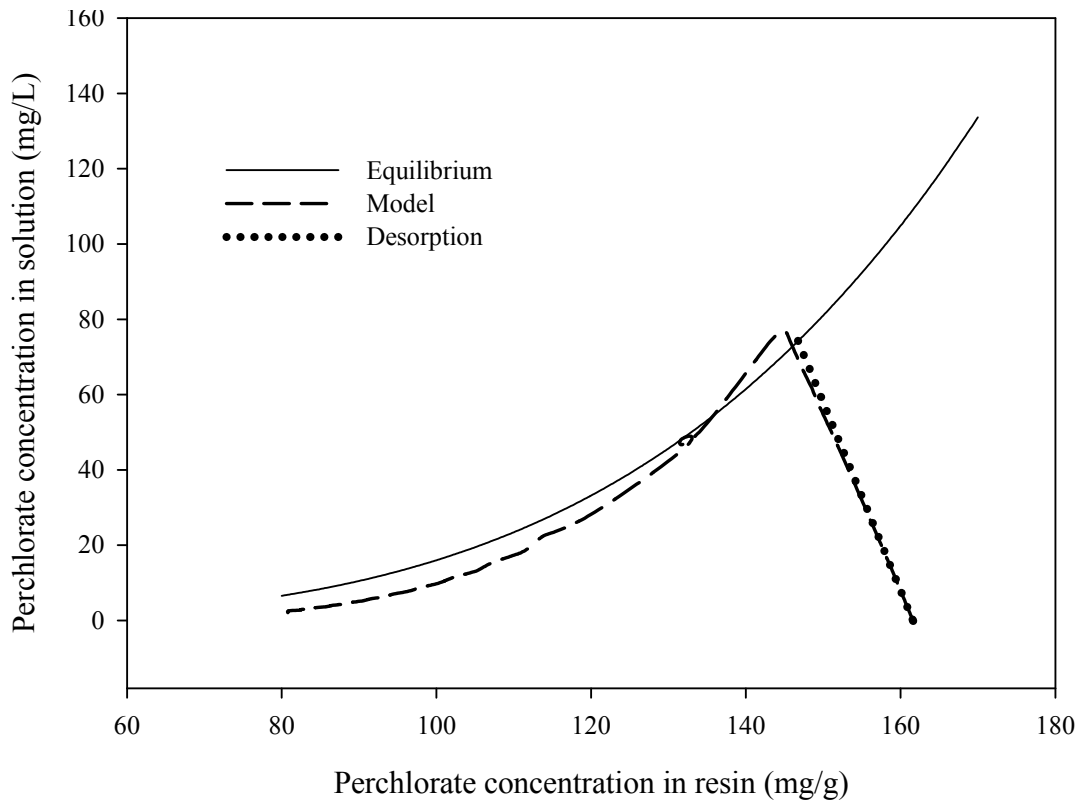


Figure 4-29 Operating diagram of the modeled biological regeneration of perchlorate desorbed from the resin.

One way of improving the desorption and biological regeneration process would be to change the slope of the operating line. By increasing the volume of the solution, the slope would decrease and the driving force ($q_o - q_e$) would increase. More perchlorate could be desorbed in this way, which in turn would increase the biomass and the rate of biodegradation. An increased biodegradation rate would degrade perchlorate faster and will “shift” the operating line more to the left.

A study by Tripp (2001), demonstrated that an increased in temperature (from 20°C to 60°C) improved the adsorption kinetics and also the efficiency of regeneration. It is

suggested to study the effect of increased temperature on the desorption of perchlorate and the biological regeneration of the resin inside the membrane. Hypothetically, an increase in temperature would have an effect on the chemisorption process controlling the kinetics of desorption and on the biodegradation and behavior of culture NP30.

Further research on the desorption and biological regeneration of perchlorate from the exhausted resin could be carried out in a reactor with the configuration presented in Figure 4-30. The proposed configuration includes a vessel to house culture NP30 and the membrane containing a fixed bed of the resin to be regenerated. The 6% NaCl solution can be supplied upward into the membrane for the desorption of perchlorate. Two streams can be taken from the culture side of the reactor: one for recirculation and sampling and the other one for waste.

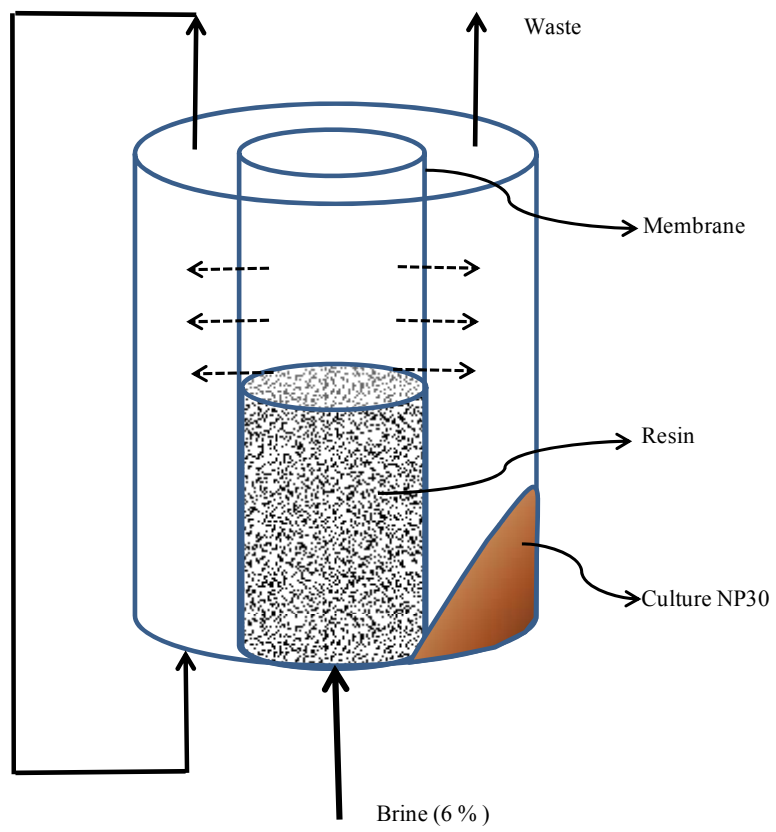


Figure 4-30 Reactor design for the biological regeneration of perchlorate exhausted resin.

CHAPTER 5 CONCLUSIONS AND FUTURE STUDY

This project studied the behavior of adsorption and desorption of perchlorate onto a strong base anion (SBA) exchange resin. Knowledge of the equilibrium, sorption kinetics and biological degradation was applied to develop a model to describe the combined process of desorption and biological regeneration of the resin.

The analysis of the results originated the following conclusions:

- The resin operating capacity estimated from breakthrough is 1.1 meq/g.
- Breakthrough of ClO_4^- occurred after approximately 5700 BV.
- The estimated capacity from a batch experiment was determined to be 1.4 meq/g of dry resin.
- Equilibrium can be described with the Freundlich isotherm model with fitted parameters $K_F = 50 \text{ (mg/g)(L/mg)}^{1/n}$ and $n = 2.36$.
- The average perchlorate-chloride separation factor is 4700 ± 1700 .
- The adsorption rate of the loose resin is higher than the adsorption rate of the resin in the membrane during the first 60 minutes.
- The desorption experiments showed a higher desorption rate of the loose resin within the first hour compared to the resin in the membrane.
- The mass transfer process for desorption is a function of the resin characteristics such as matrix type and functional groups and not the resin mass or arrangement.

- The application of several kinetic models found that intraparticle diffusion coefficients of perchlorate adsorption and desorption are of the same order of magnitude between 1.5×10^{-5} and 4.5×10^{-5} cm^2/min .
- Adsorption and desorption experimental data is best described by the pseudo-second order model, suggesting that the rate limiting stage for adsorption and desorption of perchlorate into the resin may be chemisorption.
- The pseudo second-order model predicted a rate constant of adsorption k_{p2} of 2.1×10^{-8} , 4.3×10^{-7} , and 6.4×10^{-8} for 1.00 g, 2.00 g and 3.00 g of resin respectively.
- The values of the desorption rate constants determined are -7.8×10^{-2} , -4.1×10^{-2} and -3.9×10^{-2} , for 1.00 g, 2.00 g and 3.00 g respectively.
- A model was developed for describing the biological regeneration of perchlorate desorbed from the exhausted resin inside the membrane.
- The model is sensitive to the Freundlich adsorption intensity parameter, n . A change in the value of n from 2.36 to 4.0 allowed for better simulation of the results.
- The model showed an increase in the amount of perchlorate in the solution for the first 40 minutes similar to the one obtained for samples taken at 1 hour of biological regeneration.
- A rapid decline of perchlorate concentration followed after 1 hour despite the fact that perchlorate was still being desorbed. The modeled results showed that the rate of perchlorate degradation by NP30 culture is responsible for this decline.

- The culture is capable of regenerating the exhausted resin even though is not in direct contact with it.
- A reactor designed to carry out the biological regeneration of the exhausted resin could consist of the resin placed in a tubular membrane column. The membrane would be installed in a plexiglass or glass cylindrical column containing the culture NP30.

5.1 Future Studies

Future studies including a research on the effect of temperature on the chemisorption mechanism and the behavior of the culture to regenerate the resin are recommended. It is also suggested to study the effect of decreasing the ratio of resin mass to volume of regenerant solution since it could provide valuable information for optimizing the process.

REFERENCES

- Abdullah, M.A., Chiang, L., Nadeem, M. 2009, Comparative evaluation of adsorption kinetics and isotherms of a natural product removal by Amberlite polymeric adsorbents. *Chemical Engineering Journal*. 146:370-376.
- Aldridge, L., Gillogly, T., Oppenheimer, J., Lehman, S.G., Witter, K., Burbano, A., Clifford, D., Tripp, T. 2004. Treatment of perchlorate using single use ion-exchange resins. *AWWA Research Foundation*. 43 pp.
- ATSDR (Agency for Toxic Substances and Disease Registry). 2008. *Toxicological profile for Perchlorates*. Atlanta, GA: U.S. Department of Health and Human Services. Available on the internet at: <http://www.atsdr.cdc.gov/ToxProfiles/tp162.pdf>
- Batista, J.R., Gingras, T.M., Vieira, A.R. 2002. Combining Ion-exchange (IX) technology and biological reduction for perchlorate removal. *Remediation*. Winter: 21-38.
- Baup, S., Jaffre, C., Wolbert, D., Laplanche, A. 2000. Adsorption of pesticides onto granular activated carbon: determination of surface diffusivities using simple batch experiments. *Adsorption*. 6:219-228.
- Bowman, R. 2004. New membrane reactor process effectively treats for perchlorate, nitrates. *Journal AWWA*. 64-65.

Cang, Y., Roberts, D.J., Clifford, D.A., 2004. Development of cultures capable of reducing perchlorate and nitrate in high salt solutions. *Water Research*. 38 (14-15), 3322-3330.

Chiarle, S., Ratto, M., Rovatti, M. 2000. Mercury removal from water by ion exchange resins adsorption. *Water Research*. 34(11):2971-2978.

Chung, J., Rittman, B.E., Wright, W.F., Bowman, R.H. 2007. Simultaneous bio-reduction of nitrate, perchlorate, selenate, chromate, arsenate, and dibromochloropropane using a hydrogen-based membrane biofilm reactor. *Biodegradation*. 18:199-209.

Chung, J., Shin, S., Oh, J. 2009. Characterization of a microbial community capable of reducing perchlorate and nitrate in high salinity. *Biotechnology Letters*. 31(7):959-966.

Coates, J.D., Michaelidou, U., Bruce, R.A., O'Connor, S.M., Crespi, J. N., Achenbach, L.A., 1999. Ubiquity and diversity of dissimilatory (per)chlorate-reducing bacteria. *Applied and Environmental Microbiology* 65 (12), 5234–5241.

Erdoğdu, F. 2005. Mathematical approaches for use of analytical solutions in experimental determination of heat and mass transfer parameters. *Journal of Food Engineering*. 68:233-238.

Gomes, C. P., Almeida, M. F., Loureiro, J.M. 2001. Gold recovery with ion exchange used resins. *Separation and Purification Technology*. 24:37-57.

Guo, S., Li, W., Zhang, L., Peng, J., Xia, H., Zhang, S. 2009. Kinetics and equilibrium adsorption study of lead(II) onto the low cost adsorbent-*Eupatorium adenophorum* spreng. *Process Safety and Environmental Protection*. 87:343-351.

Health Canada (September 1, 2008). *Perchlorate and human health*. Available on the internet at: <http://www.hc-sc.gc.ca/ewh-semt/pubs/water-eau/perchlorate-eng.php>

Hiremath, T., Roberts, D.J., Lin, V., Clifford, D.A., Gillogly, T.E.T., Lehman, S.G. 2006. Biological treatment of perchlorate in spent ISEP ion-exchange brine. *Environmental Engineering Science*. 23(6):1009-1016.

Ho, Y.S. 2006. Review of second-order models for adsorption systems. *Journal of Hazardous Materials*. B136:681-689.

Ho, Y.S., McKay, G. 1999. The sorption of lead(II) ions on peat. *Water Research*. 33:578-584.

Ho, Y.S., Ng, J.C.Y., McKay, G. 2010. Kinetics of pollutant sorption by biosorbents: Review. *Separation and Purification Methods*. 29(2):189-232.

Hristovski, K., Westerhoff, P., Möller, T., Sylvester, P., Condit, W., Mash, H. 2008. Simultaneous removal of perchlorate and arsenate by ion-exchange media modified with nanostructured iron (hydr)oxide. *Journal of Hazardous Materials*. 152:397-406.

Hungate, C. 1969. The anaerobic mesophilic cellulolytic bacteria. *Bacteriology*. 14, 1.

ITRC (Interstate Technology and Regulatory Council). 2008. *Remediation technologies for perchlorate contamination in water and soil*. Washington, D.C. Interstate technology and Regulatory Council, Perchlorate team.

Kashyap, V. 2006. Biological regeneration of perchlorate loaded strong base anion resins. M.Sc. Thesis, Civil and Environmental Engineering, University of Houston.

Koopal, L. K., Avena, M. J. 2001. A simple model for adsorption kinetics at charged solid-liquid interfaces. *Colloids and Surfaces A: Physicochemical and Engineering Aspects*. 192:93-107.

Kumar, P. S., Ramalingam, S., Kirupha, D., Murugesan, A., Vidhyadevi, T., Sivanesan, S. 2011. Adsorption behavior of nickel(II) onto cashew nut shell: Equilibrium, thermodynamics, kinetics, mechanisms and process design. *Chemical Engineering Journal*. 167:122-131.

Lehman, S.G., Badruzzaman, M., Adham, S., Roberts, D.J., Clifford, D.A. 2008. Perchlorate and nitrate treatment by ion exchange integrated with biological brine treatment. *Water research*. 42:969-976.

Lide, D. 2006. CRC Handbook of chemistry and physics, 87th ed. Talor and Francis Group, Boca Raton, Floorida.

Lin, X., Robertrs, D. J., Hiremath, T., Clifford, D., Gillogly, T., Lehman, G. 2007. Divalent cation addition (Ca^{2+} or Mg^{2+}) stabilizes biological treatment of perchlorate and nitrate in ion-exchange spent brine. *Environmental Engineering Science*. 24:725-732

Matos, C.T., Velizarov, S., Crespo, J.G., Reis, M.A.M. 2006. Simultaneous removal of perchlorate and nitrate from drinking water using the ion exchange membrane bioreactor concept. *Water Research*. 40:231-240.

Motzer, W.E. 2001. Perchlorate: problems, detection, and solutions. *Environmental Forensics*, 2(3):301-311

MWH (Montgomery Watson Harza). 2005. *Water Treatment Principles and Design*. 2nd ed. John Wiley and Sons, Inc.

OEHA (Office of Environmental Health Hazard assessment of California). 2009. *Public Health Goals (PHG)*. Available on the internet at: <http://www.oehha.ca.gov/water/phg/perchphg31204.html>

Perry, H.R., Green, D.W. 1999. Perry's Chemical Engineerings' Handbook. The McGraw-Hill Companies Inc.

Plazinski, W., Rudzinski, W. 2010. A novel two-resistance model for the description of the adsorption kinetics onto porous particles. *Langmuir*. 26(2):802-808.

Qui, H., L V, L., Pan, B., Zhang, Q. J., Zhang, W. M., Zhang, Q. X., 2009. Critical review in adsorption kinetic models. *Journal of Zhejiang University Science A*.10(5):716-724.

Shek, T. H., Ma, A., Lee, V. K. C., McKay, G. 2009. Kinetics of zinc ions removal from effluents using ion exchange resin. *Chemical Engineering Journal*. 146:63-70.

Sonetaka, N., Fan, H., Kobayashi, S., Chang, H., Furuya, E. 2009. Simultaneous determination of intraparticle diffusivity and liquid mass transfer coefficient from a single-component adsorption uptake curve. *Journal of Hazardous Materials*. 164:1447-1451.

Sutton, P.M. 2006. Bioreactor configurations for ex-situ treatment of perchlorate: A review. *Water Environment Research*. 78(13):2417-2427.

Tripp, A.R. 2001. Selectivity considerations in modeling the treatment of perchlorate using ion exchange processes. Ph.D. Thesis, Civil and Environmental Engineering. University of Houston.

Tripp, A.R., Clifford, D.A. 2006. Ion exchange for the remediation of perchlorate-contaminated drinking water. *Journal AWWA*. 98(4):105-114.

United states Environmental Protection Agency (US EPA). 2005a. *Perchlorate and perchlorate salts*. Available on internet at: <http://www.epa.gov/iris/subst/1007.htm>

United States Environmental Protection Agency (US EPA). 2009. *Interim Drinking water health advisory for perchlorate*. Available on internet at: http://www.epa.gov/ogwdw000/contaminants/unregulated/pdfs/healthadvisory_perchlorate_interim.pdf

Urbansky, E. T. 2002. Perchlorate as an environmental contaminant. *Environmental Science and Pollution Research*. 9(3):187-192.

Urbansky, E.T. 1998. Perchlorate chemistry: implications for analysis and remediation. *Bioremediation Journal*. 2:81-95.

Urbansky, E.T., Brown, S.K., Magnuson, M.L., Kelty, C.A. 2001. Perchlorate levels in samples of sodium nitrate fertilizer derived from Chilean caliche. *Environmental Pollution*. 112:299-302.

Urbansky, E.T., Magnuson, M.L. 2000. Sensitivity and selectivity enhancement in perchlorate anion quantitation using complexation-electrospray ionization-mass spectrometry. *Perchlorate in the Environment*. Kluwer Academic/Plenum, New York, NY. Chapter 8.

Van Ginkel, S.W., Ahn, C.H., Badruzzaman, M., Roberts, D.J., Lehman, G., Adham, S.S., Rittman, B.E. 2008. Kinetics of nitrate and perchlorate reduction in ion-exchange brine using the membrane biofilm reactor (MBfR). *Water Research*. 42:4197-4205.

Venkatesan, A. K., Sharbatmaleki, M., Batista, J. R. 2010. Bioregeneration of perchlorate-laden gel-type anion-exchange resin in a fluidized bed reactor. *Journal of Hazardous Materials*. 117:730-737.

Wang, C., Lippincott, L., Yoon, I.H., Meng, X. 2008. Modeling, rate-limiting step investigation, and enhancement of the direct bio-regeneration of perchlorate laden anion-exchange resin. *Water Research*. 43:127-136.

Washinski, A.M., Etzel, J.E. 1997. Environmental ion exchange, principles and design. CRC Press LLC, Boca Raton, Fla.

- Xiao, Y., Roberts, D.J., Zuo, G., Badruzzaman M., Lehman G.S. 2010. Characterization of microbial populations in pilot-scale fluidized-bed reactors treating perchlorate- and nitrate-laden brine. *Water Research*. 44:4029-4036.
- Xie, Y., Li, S., Wang, F., Liu, G. 2009. Removal of perchlorate from aqueous solution using protonated cross-linked chitosan. *Chemical Engineering Journal*. 156:56-63
- Xiong, Z.; Zhao, D.; Harper, Jr. W.F. 2007. Sorption and desorption of perchlorate with various classes of ion exchangers: A comparative study. *Ind. Eng. Chem. Res.* 46, 9213.
- Yoon, I.H., Meng, X., Wang, C., Kim, K.W., Bang, S., Choe, E., Lippincott, L. 2008. Perchlorate adsorption and desorption on activated carbon and anion exchange resin. *Journal of Hazardous Materials*, 164:87-94.
- Yovanovich, M.M. (August 2010). *Simple Explicit Expressions for Calculation of the Heisler-Grober Charts*. Available at http://www.mhtlab.uwaterloo.ca/pdf_papers/mht196-8.pdf.
- Zorzano, M.P., Mateo-Marti, E., Prieto-Ballesteros, O., Osuna, O., Renno, N. 2009. Stability of liquid saline water on present day Mars. *Geophysical Research Letters*. 36(20):L20201.
- Zuo, G. 2008. Kinetics and microbial ecology of two salt-tolerant perchlorate reducing enrichment cultures. Ph.D. Thesis, Civil and Environmental Engineering. University of Houston.

APPENDIX A

Sample of spreadsheet model calculation of desorption and biological regeneration of perchlorate from single use SBA

Time min	qn+1 mg/g	qe mg/g	Ce Freundlich	Ce Balance	qe mg/g	t/q min g/mg	qn mg/g	S mg/L	X mgVSS/L	v (mg/mg/min)	S biodegraded mg/L	C left mg/L	qo mg/g
0	161.6	140.6	104.9	104.9	140.6	0.0312	161.6	0.00	4159.0	0.0000	0.000	0.00	161.60
5	161.6	140.6	104.9	104.9	140.6	0.0312	160.3	6.69	4159.4	0.0122	0.061	6.63	161.59
10	160.3	139.8	102.2	102.2	139.8	0.0315	158.5	15.23	4160.3	0.0220	0.220	15.01	161.54
15	158.5	138.8	98.8	98.8	138.8	0.0320	156.4	25.52	4161.8	0.0295	0.443	25.07	161.45
20	156.4	137.5	94.8	94.8	137.5	0.0325	154.0	37.25	4164.1	0.0351	0.703	36.54	161.31
25	154.0	136.0	90.2	90.2	136.0	0.0330	151.3	49.95	4167.1	0.0393	0.982	48.96	161.12
30	151.3	134.3	85.2	85.2	134.3	0.0337	148.5	63.05	4170.9	0.0423	1.270	61.78	160.86
35	148.5	132.5	80.2	80.2	132.5	0.0343	145.7	76.01	4175.4	0.0446	1.561	74.45	160.55
40	145.7	130.6	75.3	75.3	130.6	0.0350	142.9	75.25	4179.9	0.0445	1.781	73.47	145.30
45	130.6	120.2	51.9	51.9	120.2	0.0373	134.0	51.86	4183.0	0.0399	1.797	50.06	130.25
50	120.2	112.5	38.5	38.5	112.5	0.0380	131.7	50.06	4186.1	0.0395	1.975	48.09	129.86
55	120.2	112.5	38.5	38.5	112.5	0.0378	132.2	48.09	4188.9	0.0390	2.143	45.94	129.43
60	112.5	106.5	30.1	30.1	106.5	0.0417	120.0	30.07	4190.7	0.0322	1.933	28.14	125.63
65	106.5	101.7	24.4	24.4	101.7	0.0439	113.9	24.36	4192.2	0.0291	1.889	22.47	118.36
70	101.7	97.6	20.3	20.3	97.6	0.0449	111.4	20.28	4193.4	0.0263	1.844	18.44	115.08
75	97.6	94.1	17.2	17.2	94.1	0.0466	107.3	17.25	4194.5	0.0240	1.798	15.45	110.42
80	94.1	91.2	14.9	14.9	91.2	0.0475	105.2	14.92	4195.3	0.0219	1.754	13.17	107.84
85	91.2	88.5	13.1	13.1	88.5	0.0489	102.2	13.09	4196.1	0.0201	1.712	11.38	104.43
90	88.5	86.2	11.6	11.6	86.2	0.0498	100.4	11.61	4196.8	0.0186	1.671	9.94	102.39
95	86.2	84.1	10.4	10.4	84.1	0.0510	97.9	10.40	4197.5	0.0172	1.633	8.77	99.70
100	84.1	82.3	9.4	9.4	82.3	0.0518	96.5	9.40	4198.0	0.0160	1.598	7.80	98.05
105	82.3	80.6	8.6	8.6	80.6	0.0530	94.4	8.55	4198.5	0.0149	1.564	6.99	95.83
110	80.6	79.0	7.8	7.8	79.0	0.0536	93.2	7.83	4199.0	0.0139	1.532	6.30	94.48
115	79.0	77.5	7.2	7.2	77.5	0.0547	91.4	7.20	4199.4	0.0131	1.502	5.70	92.57
resin. 120	77.5	76.2	6.7	6.7	76.2	0.0553	90.4	6.66	4199.8	0.0123	1.474	5.19	91.47

APPENDIX B

Calibration curve to the perchlorate selective electrode probe, samples in 0.6 %

NaCl.

